Dear Kenny Matsuoka,

We are very appreciative for the reviews of our manuscript "Antarctic Ice Shelf Thickness Change from Multi-Mission Lidar Mapping." In response to the reviewer comments, we have revised the manuscript to clarify some essential points and add a comparative analysis with Adusumilli et al. (2018). The modifications did not change the overall conclusions or results.

In the revision, we include:

1. A point-by-point response to the reviewer comments. Responses are *italicized and gray*.
2. An enumerated list of the modifications made to the manuscript.
3. A copy of the manuscript with the changes noted. (Highlighted with ~~red struck-through text~~ to denote subtractions and blue underlined text to denote additions)
4. A final copy of the manuscript with those same changes incorporated.

Regards,
Tyler C. Sutterley

First Reviewer Comments:

This manuscript reports on estimates of thickness change and basal-melt rates along airborne survey lines over West Antarctic and Antarctic Peninsula ice shelves. These estimates were derived from lidar measurements (of surface height change) obtained from NASA's airborne campaigns between 2002 and 2015, combined with available surface velocity data from MEaSUREs/NSIDC, and surface-mass-balance and firn state information from models (RACMO2.3, and a firn-densification model). The manuscript focuses on the methodology to invert height-change measurements from airborne lidar to basal-melt estimates in a Lagrangian framework. Finally, a brief discussion on the Lagrangian vs Eulerian approaches is presented, as well as putting in context some of the ice-shelf melt-rate values obtained. I believe the results of this manuscript are of great value for comparing and calibrating satellite-derived estimates of ice-shelf thickness change and melt rates. The authors put considerable effort to integrate all available/usable NASA airborne lidar data over the West Antarctic ice shelves. While these data set is quite sparse (only available along flight lines and with a few repeats), there are still very little data available to compare against the vast amount of satellite measurements, which makes this work of particular interest to the remote-sensing community. I have, however, several questions and suggestions that I would like to see addressed prior considering publication (see comments below). Overall, the manuscript is well written and the figures are of good quality.

> *Thank you. We appreciate the thoroughly beneficial review of our manuscript. We address your comments point-by-point and update the manuscript accordingly.*

General comments:

I feel a thorough error assessment on derived melt-rate estimates is lacking. Given that, as mentioned in the manuscript itself, this set of estimates is expected to serve as a reference for published and future (e.g. from ICESat-2) satellite-derived estimates, I would expect a more comprehensive error assessment: How close to (available) in-situ measurements are these values?

> *We expanded upon our error calculation in the manuscript. There are tide gauges around Antarctica that are used for validating the CATS2008 model. The 5.5km SMB models are validated against Operation IceBridge snow radar observations, satellite melt observations, and and in-situ observations (Kuipers Munneke et al., 2017; Lenaerts et al., 2018).*

What are realistic confidence intervals given that some of the information comes from models?

> *This is an excellent question. We assume a 15% uncertainty in surface mass balance and firn height following estimates from Kuipers Munneke et al. (2017). Tidal uncertainties are estimated using the constituent RMS values from King et al. (2011). Uncertainties in flux divergence were estimated using annually resolved velocity maps (Mouginot et al., 2017a) and uncertainties in Bedmap2 ice thickness (Fretwell et al., 2013).*

How sensitive are the estimated melt-rate values to unaccounted processes (due to lack of data or knowledge)?

> *Great question. Because the ice shelves are largely in hydrostatic equilibrium, any uncertainty in terms of elevation will be magnified by approximately 10$\times$ in the final estimates of thickness change and basal melt rate.*

Some of the short-time-scale (2 to 5 years) estimates are likely subject to the large interannual-to-decadal variability characteristic in the AS-BS sector (e.g. Paolo et al. (2015)). For example, it has been shown that even ICESat-derived estimates (5-year period) can disagree substantially from longer-timescale averages (as those derived from radar altimetry). In many cases, the ICESat short time span (Pritchard et al. (2012); Rignot et al. (2013)) overestimate the underlying decadal trend, simply because their estimates are focusing on the more variable short-term scales.

Absolutely. At present, records from laser altimetry are far less compete than records from radar altimetry in terms of temporal resolution and duration (Paolo et al., 2015; Adusumilli et al., 2018). However, laser altimetry datasets have more accurate surface determination and can more accurately track over regions of abrupt topographical change. ICESat-2 should provide a valuable extension to the laser altimetry record and help separate short-term oscillations with long-term change.

Substantial (and important) information on the methodology is being introduced in the Discussion section of the manuscript. I understood some aspects/limitations of the methodology only after reaching the discussion page (which is the final portion of the Main text).

Good point. Text and figures have been reordered for improved continuity and presentation.

Can direct comparisons with previously published estimates be made for some locations (using, for example, Pritchard et al. (2012); Rignot et al. (2013); Paolo et al. (2015) and Adusumilli et al. (2018)? This would be very valuable and could motivate good discussion regarding discrepancies and/or similarities.

Great point. We have added a direct comparison with the results from Adusumilli et al. (2018) and have added points emphasizing this purpose of our dataset. We did not compare with data from Paolo et al. (2015) as the publicly available data is for a different time period. We did not compare with Pritchard et al. (2012) as the data is not provided in a compiled form. Rignot et al. (2013) do not provide publicly available data.

Specific comments:

p2, l3-4: "accelerated 2 to 8 times their previous flow rates"... Please define "previous", i.e., when those measurements were taken (right before 2002, or five/ten years before)?

Great point. Added that the before and after measurements were taken in 1996 and 2003. "In 2003, a year after the collapse of the Larsen B ice shelf, some tributary glaciers draining into the Weddell Sea from the Antarctic Peninsula were flowing 2–8 times their 1996 flow rates (Rignot et al., 2004). These glaciers continued flowing at accelerated rates years after the collapse (Rignot et al., 2008; Berthier et al., 2012)."

p2, l5: "surface thinning"... Are you referring to thinning of the firn layer (i.e. densification), which I don't think any of the provided references support this? Or perhaps you mean "surface lowering"?

Clarified to mean "dynamic thinning" as noted in Pritchard et al. (2009) and Flament and Rémy (2012).

p2, l7: What is an "internal change in ice dynamics" (as opposed to "an external change")?

Changed to "The dynamical change of these glaciers..."

p2, l8: ocean melt → ocean-driven melt

Done. Thank you.

p2, l25: "over Pre-IceBridge and NASA Operation IceBridge campaigns is shown"... Do you mean "prior to and during NASA Operation IceBridge campaigns is shown..."?

Changed to "The spatial coverages of each instrument in Antarctica for the campaigns prior to and during NASA Operation IceBridge are shown in Figure 1." Thank you.

p2, l27-28: What exactly do the 'converted' heights represent? Height w.r.t. an ellipsoid model or w.r.t. a geoid model. . . it seems you are tracking deviations from the geoid, and why you need this conversion? Perhaps to invert for thickness/basal melt, but it is not clear at this point in the text.

Good point. Changed to "In order to track changes in ice shelf freeboard, the ellipsoid heights for each instrument were then converted to be in reference to the GGM05 geoid using gravity model coefficients provided by the Center for Space Research (Ries et al., 2016)."

p3, l7: What is "the scale of the individual triangular facet"?

Added that an individual triangle is ∼10–100m.

p3: On "Tidal and Non-Tidal Ocean Variation": Armitage et al. (2018) showed substantial sea-level anomalies (changes w.r.t. mean sea level) around Antarctica: about 3 cm at seasonal scales and 5 cm associated with the ENSO cycle. How will these translate to/impact the derived ice-shelf height changes? At the very least, these should be accounted for in the error budget. Note that these SLAs around Antarctica could not be precisely measured until only recently (e.g. Armitage et al. (2018)). What precisely are the "Non-tidal sea surface anomalies over ice-free ocean points", i.e., what process are you removing with the CMEMS product? Is this accounting for spatially variable sea-level rise? For example, Paolo et al. (2015) corrected for rates of sea-level change around Antarctica varying from 2 to 4 mm/yr (compared to the global mean of ∼3 mm/yr)

Good point. Paolo et al. (2015) used the same dataset from AVISO in their study (described in their supplementary materials). We clarify that the sea surface anomalies removed are local sea level change, which will include long-term sea level rise and inter-annual fluctuations. We add the sentence "Regional sea levels fluctuate due to changes in ocean dynamics, ocean mass, and ocean heat content (Church et al., 2011; Armitage et al., 2018)." We also include that the sea surface anomalies are added to estimates of mean dynamic topography, which are the mean deviations of the sea surface from the geoid. "The non-tidal sea surface anomalies are added to estimates of mean dynamic topography, which is the mean deviation of the sea surface from the Earth's geoid due to ocean circulation."

p4, l8-10: What's the relevance of "highly complex topography of mountains and glacial valleys" if you are working over (relatively flat) ice shelves? I'm saying this because I haven't seen a comparison between the 27km and 5.5km SMB models against in-situ measurements specifically *over* the ice shelves, to be convinced that the higher-res product does provide a more accurate representation of SMB state over flat surfaces.

Fair point. While there is little difference for the ice shelves in the Amundsen Sea, there are some substantial differences for the ice shelves in the Weddell Sea. The major difference is how well the topography of the peninsula is resolved at 5.5km versus 27km. Resolving some downstream effects within the climate model requires the highest-possible spatial resolution topography (Datta et al., 2018). Added "The higher spatial resolution topography improves the modeling of wind-driven downstream effects over ice shelves (Datta et al., 2018)."

p4, l13-14: I'm confused here: "The absolute precision of the RACMO2.3p2 model outputs has been estimated. . . ", are you referring to the latest high-res model (the 5.5 km)? If so, why is the reference from 2006 (I assume they did not have the high-res model back then)?

The van de Berg et al. (2006) citation was for the method used for evaluation of the RACMO2 models. We updated the sentence to say that it is "following Kuipers Munneke et al. (2017) and Lenaerts et al. (2018)".

p5, l3-4: What is “basal thickness change rate”? Changes in ice-shelf thickness due to mass loss/gain at the bottom? Or. . .

Correct. It referred to changes in ice-shelf thickness due to losses at the base. We changed the maps to use two separate colorbars and show basal melt rates in meters of ice per year.

Fig 10: “The elevation change rates shown here are not corrected for oceanic or surface processes and are not RDE filtered”. . . Why not?

Fair question. The original intent was to only show the differences due to the processing method. We updated the figure to correct for ocean and surface processes and we noted that we have corrected for strain in the Eulerian-derived values. The data isn't RDE filtered in order to show the worst case of each technique (such as near the rifting that developed before the calving of the A-68 iceberg).

General comment: I don't know what 'basal thickness change means'. . . Thickness change solely due to basal mass change? Please be more specific/accurate.

Yes, this is what it referred to in the previous manuscript. All plots have been changed to show basal melt rates in terms of meters of ice per year.

p5, l33-35: Could the difference in melt rate near the grounding zone be explained simply by the (large) interannual-to-decadal variability in the AS sector (as shown, for example, by Dutrieux et al. (2014); Paolo et al. (2015); Jenkins et al. (2018))?

Yes. This point has been added to the text.

p6, l15-16: However, Lagrangian estimates miss the grounding lines due to the direction of ice flow from grounded to floating. That is, sampled sites near the grounding lines were previously over grounded ice, lacking the corresponding measurement pair for comparison. This limitation affects measurements downstream of the GL depending on time separation between data points and flow speed. Another limitation of the Lagrangian approach is the sparseness of the estimates (compared to Eulerian solutions) since not all measurements will have a matching upstream pair (as also demonstrated by Moholdt et al. (2014)). Further, in the case of airborne surveys where the flight segments do not cross the entire ice shelf, measurements on the downstream end of the transect will also lack corresponding matching pairs.

These are great points that we have been added to the methods and discussions sections.

“ In order to minimize the possibility of co-registering measurements over ice shelves with measurements over grounded ice near the grounding zone or measurements over the ocean, sea ice floes and icebergs, we only include points that are on the ice shelf for both time periods using grounded ice delineations from Rignot et al. (2016) and Mouginot et al. (2017b) and ice shelf extents manually digitized from Landsat (LPDAAC) and MODIS imagery (Scambos et al., 2001).”

p6, l18-20: Substantial smoothing was required because the effect of ice advection and divergence was not corrected for. With high-quality velocity products available today (e.g. Rignot et al. (2017); Gardner et al. (2018)) the flux-divergence signal can and should be removed (or at least reduced substantially) from the basal mass balance estimates (see for example, Berger et al. (2017); Lilien et al. (2018); Adusumilli et al. (2018)).

Excellent point. We have noted this in the text.

p6, l19-20: "spatial smoothing [. . .] to filter out the effects of advection". . . This misleading. The smoothing is not targeting specifically the advection-related features, instead, is removing everything that falls within the cutoff frequency of the smoother.

Fair point. While one of the main noise sources for ice shelves are these advected features, it is absolutely correct that the filters were not specifically used to remove these artifacts. This portion has been removed.

p6, l32-33: I think a more comprehensive "update" (to Pritchard et al. (2012)) has already been presented (see Paolo et al. (2015)). . . or not?

Fair point. While they are based on different datasets (radar vs. laser), Paolo et al. could be considered an update to Pritchard et al.. This sentence has been removed.

p7, first para: The discussion on the limited velocity coverage back in time for Lagrangian estimation is important (modern Eulerian estimates also depend on the removal of the advection signal). I feel the authors should go beyond just discussing and try and quantify the effect (i.e. the contribution to the error budget) of potential changes in ice flow. In other words, how sensitive are the melt rate estimates to changing velocity magnitudes? Typical magnitudes of velocity change can be taken from the literature for the few locations they are available (e.g. Mouginot et al. (2014)).

This is an excellent point. We include estimates of annual changes in flux divergence in our error budgets. Including time-variable velocity maps to advect the locations of the elevation measurements in our Lagrangian methodologies is the subject of future work.

Second Reviewer Comments

SUMMARY

The authors use airborne laser altimetry (from airborne topographic mappers (ATM)) over Antarctic Peninsula (AP) and Amundsen Sea (AS) ice shelves, plus models of surface mass balance and firn compaction, to measure ice shelf thinning rates and assign these rates to individual terms in the mass balance. The study is complementary to several previous studies that used satellite altimeters. The coverage of ATM is poor prior to Operation Icebridge (OIB). However, it has some advantages in terms of dedicated tracks, in particular allowing measurements to get close to grounding lines. It is therefore a valuable study, and dataset, to provide to the community.

Note that I have read the comments by Anonymous Referee #1 and agree with most of inverse barometer) is a bigger source of error especially given that the ATM missions are essentially instantaneous, and sparse in time.

We are really appreciative for the helpful review of our manuscript. In response, we have revised the manuscript and clarified some essential points.
We completely agree that other sources of oceanic variability can influence the measurements over ice shelves. In the current and previous versions of the manuscript, sea level variations are accounted for using AVISO products distributed by Copernicus. The use of these sea level anomaly products follows the ice shelf work of Paolo et al. (2015).

GENERAL

1. I spent a lot of the paper being confused by the term "ice thickness change rates". This relates to the use of Lagrangian calculations. The authors explain why they use Lagrangian methods, which makes sense, although it often seems to lead to massive data loss: compare figure 1 flight lines with locations of ice thickness change on figures 5, 7, 8 and 9. However, Lagrangian methods are really just a tool to get the mass balance terms. The most important thing is whether the ice shelf is losing mass, and the spatial distribution of that loss, so that Eulerian variability is really what you want to report in terms of SMB, BMB and divergence.

   Figures and text have been changed to use basal melt rates (in terms of meters of ice equivalent per year). The data is spatially sparse over ice shelves regardless of reference frame (especially in the pre-IceBridge era). After 2009, it is possible to have nearly annually resolved estimates of ice thickness change along the flight lines for some ice shelves. Idealistically, reporting Eulerian variability would be preferable over Lagrangian variability. However, substantial smoothing or averaging is required with Eulerian-derived estimates to reduce the impact of noise, and thus Lagrangian-derived estimates can provide more accurate solutions if the spatial coverage isn't comprehensive.

   If you agree with that, then the important "ice thickness change rate" is Eulerian, which you get back from Lagrangian by adding back in the strain thinning and advection terms. (If they appear to be changing, that's relevant too.) The simplest approach to clarify what you're reporting would be to introduce Eulerian and Lagrangian rate symbols early (d/dt and D/Dt), then use the symbol rather than the words. Every time I see capital 'D', I'll know it is Lagrangian.

   Nomenclature has been updated.

2. It is strange that Results are presented first, then back to Methods, as far as figures go. Given how much the data distribution thins out from Fig. 1 to the Lagrangian maps, the first thing to do would

be to determine if Lagrangian is a good method. Potentially, you are better off with averaging of a lot of noisy Eulerian measurements rather than far fewer cleaner Lagrangian values. I'd move Fig. 6 to Fig. 5, demonstrating the value of along-flowline repeat ATM, then next I'd have something like Figure 10 to make points about the value of Lagrangian vs Eulerian. You need to also check that you are comparing the same things here: results from Eulerian TINs should be the same average as Lagrangian TINS provided the Lagrangian values have been re-corrected for advection and strain.

Thank you. The figures and text have been reordered for improved continuity. We include that the Eulerian-derived values are corrected for the effects of advection following Moholdt et al. (2014). As mentioned in the manuscript, we have results for all available Operation IceBridge data in an Eulerian reference frame using a similar TINs-based methodology. You are absolutely correct that there is more available data when computed in an Eulerian frame of reference; however, the data is still spatially sparse over ice shelves (particularly in the pre-IceBridge era). Mission priorities have limited measurements over ice shelves until fairly recently (when Mag/Grav measurements have enabled improved estimations of sub-shelf bathymetry). The strength of the airborne laser altimetry data lies in its accurate measurements at relatively small spatial scales compared to radar altimetry data, repeatable processing methods, and ability to follow glacier flowlines.

3. The authors should look at another Cryosphere Discussions paper by Shean et al. (2018) `https://www.the-cryosphere-discuss.net/tc-2018-209/`, where Pine Island melt rates are assessed using high-res image-based Lagrangian processing.

   We are looking forward to the publication of the Shean et al. paper as it is a very complementary work that uses an independent dataset. As the paper is not presently through peer-review, we have only included citations to the Discussions paper in anticipation of a future acceptance.

4. The authors should probably compare their results for Larsen C with the ATM measurements presented in Adusumilli et al. (2018).

   Done. Figure and text have been added.

5. Overall, I think this paper fails to exploit the key features of ATM vs satellite-based products. Satellite altimeters and stereo imagery (Shean et al. (2018), and an earlier Dutrieux et al. (2014) paper), make the process easier, but all satellite altimeters lack spatial resolution and radar altimeters struggle near grounding lines and other steep regions. Think about the new science that is available from a carefully compiled ATM data set where all the biases have been corrected for. If there is no new science, the data set is still valuable as it provides independent estimates to compare with the satellite-derived values. In this case, the most obvious value of the data set is as intended for OIB: a continuation of the ICESat laser altimeter record. Why not look at ICESat data as a third, earlier period in the various plots that compare pre-2011 and post-2011 data?

   We expand upon the purpose of this paper and the benefits of having an airborne lidar derived dataset for the validation of satellite datasets and model outputs. We are investigating processes that can be derived with the airborne dataset but are leaving that for a future work. A comparison of Operation IceBridge with ICESat laser altimetry is certainly possible if a compiled dataset was publicly available. We have added a comparison with the published radar altimetry estimates from Adusumilli et al..

MAJOR: SPECIFIC

p.1/l.2: See general comments. The reader needs to know whether you mean Lagrangian or Eulerian ice thickness change, and if the Lagrangian estimates have been re-corrected back to Eulerian.

Emphasis has been added to clarify that these are Lagrangian estimates.

p.1/l.8-9: Comments on Larsen C depend on the quality of the SMB and firn models. This sentence suggests that the ice thickness change really is DH/dt, not dh/dt.

Yes, most of the estimates in this work are Lagrangian-derived ice thickness change. Also, in any reference frame, the conversion from volume to mass will be an important aspect. We added an additional sentence noting how SMB uncertainties will directly impact the basal melt rate estimate.

p.1/l.9-11: I don't think *you* show that Wilkins depends on "short time-scale and upper-ocean processes": the only evidence I see for this is citations to previous work.

Fair point. Attempting to quantify the effects of individual processes is the subject of some future work.

p.1/l.11-12: Again, this is where you'd be better off reporting dH/dt, even if you're deriving it via re-corrected DH/Dt. I was surprised that PIG was "thinning" by 40 m/yr, even close to the grounding line. The more important numbers are in comparisons: you want to show actual Eulerian thinning (dH/dt), BMB, and maybe the ice divergence term.

To clarify, we are reporting Lagrangian thickness change rates and melt rates of the Pine Island Ice Shelf and not Pine Island Glacier. Shean et al. (2018) present very similar numbers for the Pine Island Ice Shelf over similar time periods.

p.2/l.31: The Shean et al. (2018) TCD paper is another example of Lagrangian processing.

The Shean et al. paper is an excellent example of a similar methodology and a very complementary to our own work. Citation has been added.

p.3/l.27-29: I don't understand how you remove non-tidal ocean height change for ice-free ocean points from ice-shelf data. Extrapolate under the ice front? Do you get AVISO sea surface height all the way to the ice fronts at all times of ATM surveys, or does sea ice get in the way? What processes do you think the AVISO products are correcting for, or is this a coarse approximation for regional sea level rise?

Yes, it is simply an extrapolation and is a coarse approximation for regional sea level rise. The extent varies based on sea ice. We chose to use a measured estimate in order to include processes that can deviate strongly from the global ocean averages, such as steric effects and self-attraction and loading effects. The use of this correction follows Paolo et al. (2015) that used the same dataset.

p.4/l.20 ff: You need to explain all the terms in this equation immediately.

Great point. We've expanded upon each of the terms.

p.5-6 (Results): This would be clearer if you used sub-headers for each ice shelf that you are considering: Larsen C, Wilkins, Pine Island, and Dotson/Crosson. Also, this is a critical place to use symbols regarding ice thickness change: is it Eulerian dH/dt, Lagrangian DH/Dt, or Lagrangian-derived Eulerian dh/dt?

Great suggestion. The results section has been now partitioned into subsections. We added emphasis to note that all results are in a Lagrangian reference frame and the use of the Eulerian frame was for comparison purposes only.

p.5/l.27-28: Sentence starting "These periods" suggest that RACMO2.3p2 ASE055 is only available for specific periods, which then determine the breakdown of ATM into different epochs. Is this true? Regardless, the reader needs to know the period for which this high-res surface processes model is available.

Great point. We added the range of each climate simulation. "We use 5.5km horizontal resolution outputs from a 1979–2016 climate simulation of the Antarctic Peninsula (XPEN055, van Wessem et al., 2016) and a 1979–2015 climate simulation of West Antarctica (ASE055, Lenaerts et al., 2018)."

p.5/l.32-33: Rignot and Jacobs (2002) is not the right cite for "highest impact on glacial flow dynamics". They just assume that and use it to justify looking at melt rates near the grounding line. There are many more recent papers that might be relevant, e.g., Walker et al. (2007), Gagliardini et al. (2010), probably others.

Fair point. We include citations to updated and more relevant work.

p.6/l.3: Rignot (2002) seems like a strange single choice for citation here.

We expand upon this sentence and add reference to more updated work.

p.6/l.4-13: The Dotson/Crosson data are incredibly sparse, which I assume is a consequence of using Lagrangian processing given data density on Fig. 1. So (a) is this a place where higher noise in Eulerian would have been better? (b) Maybe you haven't enough data to learn whether conditions are different from the ICESat-era results of Khazendar et al. (2016)? This points again to using the ICESat-era results as a natural comparison for the more recent ATM.

Spatial sparseness at Dotson/Crosson is largely due to the availability of coincident data and not as much of a function of Eulerian versus Lagrangian reference frames. The plot below shows the same time period as the figure in the main text, but uses an Eulerian approach. Khazendar et al. (2016) used the ICESat/OIB data from Sutterley et al. (2014) as an estimate over the grounded ice and estimates from radar depth sounding and ATM over ice shelves. Creating estimates from ICESat would certainly be possible but we believe outside the purview of this paper.

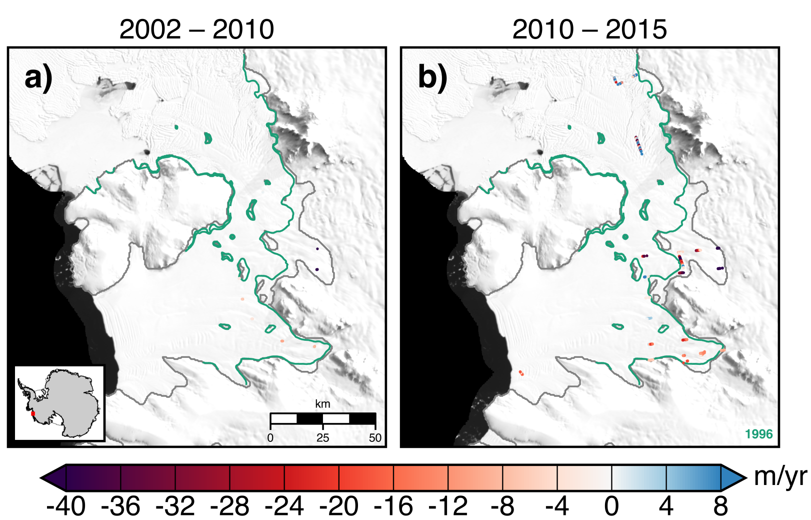

p.6/l.17: The statement "Our Eulerian approach" seems to contradict everything you've said about using a Lagrangian approach. This comparison should be much earlier in "Methods", then you could mention "We began by calculating…using three approaches, …, …, and …, applied to Larsen C. Results (Fig. X) demonstrate that…" Just make sure the figure really does compare Eulerian with re-corrected Lagrangian, or advection-and-strain-corrected Eulerian with Lagrangian.

Text and figures have been reordered for improved continuity and for the clarification of points. We also clarify that the Eulerian values are corrected for advection and strain effects.

p.6/l.26-27: Dotson/Crosson data are extremely sparse, and it isn't at all clear that Lagrangian methods are the best approach here.

The lack of data at Dotson/Crosson is more due to the lack of coincident flight lines over the ice shelf. This point has been emphasized.

p.6/l.29-30: the statement "would likely not be representative" is probably true, especially for Dotson/Crosson, but needs to be justified, e.g., on the basis of data sparseness.

Point added.

p.6/l.30-32: It isn't really obvious why you need a DEM, specifically from photogrammetry, to use ICESat-2 for dH/dt. It helps with the advection terms and Lagrangian TINs, but maybe you need to set up the idea better, along the lines of "The Lagrangian method is strongly dependent on a detailed understanding of surface topographic features being advected by the ice flow…"

Absolutely correct that digital elevation models are not necessary for deriving elevation change with ICESat-2, particularly in an Eulerian reference frame. Lagrangian reference frames are more difficult, particularly if the ice shelf flow is roughly perpendicular to the satellite tracks, such as in the Antwitharctic peninsula. DEMs would improve the tracking of ice parcels, and decrease data "loss" between different satellite tracks. These points have been clarified in the text. Thank you for the comment.

p.7/l.13-22: (a) This section does not flow well, but it does raise two issues that you haven't really explained well up to now:

a) Pros and Cons of radar vs laser. The goal, probably, is change in vertically integrated *mass* (or ice-equivalent thickness). With laser, you get true surface height really well, but conversion to mass depends on the firn model. If the snow layer is lighter than you thought, you infer too much mass. With radar, it is complicated by penetration (and footprint size), but on the other hand maybe that's good because the inferred reflecting surface is below the lightest snow. However, you still need the model of firn compaction below the reflector.

   Good point. We expand upon the strengths and weaknesses of each dataset. We include a more detailed description of the complications for detecting ice shelf surface height from each dataset.

b) The study hasn't really been set up as well as it could have. This gets back to: Is there really new scientific insight here, or is the goal mainly to provide an independent data set that is of specific value in comparing with satellite-derived ice-shelf changes, specifically laser-based? Either way is good for a paper, with the latter being the justification for OIB anyway. A clearer goal, stated early, might help organize the paper so that results are written around that goal. At the moment the paper reads like you're identifying new science, but the

Results section mainly relies on, or repeats, previous studies, just with a new data set. e.g., Adusumilli et al. (2018) reach the same conclusions regarding Larsen C, except they don't spend much time of the advection and-strain terms, but they do use ATM as validation. Wilkins is interesting, but why not compare ATM tracks with ICESat to get a better sense of pre- and post-ICESat behavior?

Fair point. We expand upon the justification of the research and the manuscript in the introduction. We clarify the purpose of the work and justification of using Operation IceBridge data. Creating a comparable dataset using data from the original ICESat mission is worthwhile and certainly possible; however, we believe outside the purview of this manuscript. We include a comparison with the Adusumilli et al. dataset over the Larsen-C ice shelf. We are working towards the overarching goals of ice-ocean interaction and the downstream effects on the grounded ice. We will also have more in depth interpretation of the results for particular ice shelves in future work.

TECHNICAL: SPECIFIC

p.1/l.19-20: (a) I think Rignot et al. (2013) just assumes that ice shelves buttress grounded ice, don't show it. You can't cite every paper that makes that claim. (b) Sentence starting "The thinning..." just repeats the idea of buttressing.

The buttressing effect of ice shelves is fairly well documented and we include citations to modeling efforts to quantify the effect.

p.2/l.1-2: Again, you're repeating the buttressing argument.

The purpose of this second sentence is to emphasize how changes in ice shelves affect the grounded ice.

p.2/l.19: Abbreviation "WFF" isn't used again, so not needed.

Done. Thank you.

p.2/l.32: Here you cite Rignot et al. (2017) for MEASURES, but on p.4/l.24 it is Mouginot et al. (2017a).

This has been fixed. Thank you. The Mouginot et al. (2017a) data was used to calculate deviations from mean ice flow.

p.4/l.28: This reads like the range of validity for hydrostatic is only the narrow band of 1-8 km from the grounding line. You mean that this region is *not* hydrostatic, but that the flexural boundary width is in this range.

Correct. The intent was to describe regions downstream of the 1–8 km wide grounding zones. Changed to "The ice thickness estimates are calculated assuming hydrostatic equilibrium, which should be valid for most areas downstream of the 1–8 km wide grounding zones (Brunt et al., 2010, 2011)."

General style, especially in Results: You make a habit of starting paragraphs with "Figure X shows...". This sounds like you have a collection of figures to describe, rather than making figures to fit your narrative.

General style has been updated to first describe each ice shelf and introduce results.

General Style: "{Name} ice shelf" or "{Name} Ice Shelf"?

Updated. Thank you for the suggestion.

p.6/l.2: Why refer to Fig. 8*b*, specifically?

Fair point. This has been fixed. Thank you.

p.6/l.5: I think this means "two periods – 2002-2010 and 2010-2015 – are shown in"

Precisely. Thank you.

p.7/l.8: more precisely "maps of time-varying velocity"

Changed to "time-variable velocity maps"

p.7/l.9-12: Would be good to have cites to each of these products.

Citations added.

List of Changes

1. *Modified* "We calculate ice thickness change rates in a Lagrangian reference frame to reduce the effects from advection of sharp vertical features, such as cracks and crevasses, which can saturate Eulerian-derived estimates." *to* "The ice thickness change rates are calculated in a Lagrangian reference frame to reduce the effects from advection of sharp vertical features, such as cracks and crevasses, that can saturate Eulerian-derived estimates."

2. *Modified* "We use our method over different ice shelves in Antarctica, which vary in terms of the processes that drive their change, their size and their repeat coverage but are all susceptible to short-term changes in ice thickness." *to* "We use our method over different ice shelves in Antarctica, which vary in terms of size, repeat coverage from airborne altimetry and dominant processes governing their recent changes."

3. *Modified* "Larsen-C ice shelf" *to* "Larsen-C Ice Shelf"

4. *Modified* "Wilkins ice shelf" *to* "Wilkins Ice Shelf"

5. *Modified* "At The Pine Island ice shelf in the critical region near in the grounding zone, we find that ice shelf thinning rates exceed 40 m/yr. The thickness change is dominated by strong submarine thinning." *to* "At the Pine Island Ice Shelf in the critical region near in the grounding zone, we find that ice shelf thinning rates exceed 40 m/yr with the change dominated by strong submarine melting."

6. *Modified* "Dotson and Crosson ice shelves" *to* "Dotson and Crosson Ice Shelves"

7. *Added* "Operation IceBridge provides a validation dataset for floating ice shelves at moderately high resolution when co-registered using Lagrangian methods."

8. *Modified* "After the 2002 collapse of the Larsen B ice shelf, some tributary glaciers draining into the Weddell Sea from the Antarctic Peninsula accelerated 2 to 8 times their previous flow rates, and continued flowing at accelerated rates years after the collapse (Rignot et al., 2004, 2008; Berthier et al., 2012)." *to* "In 2003, a year after the collapse of the Larsen-B Ice Shelf, some tributary glaciers draining into the Weddell Sea from the Antarctic Peninsula flowed at rates 2–8 times their 1996 flow rates (Rignot et al., 2004). These glaciers continued flowing at the accelerated rates years after the collapse (Rignot et al., 2008; Berthier et al., 2012)."

9. *Modified* "Glaciers of the Amundsen Sea Embayment (ASE) in West Antarctica have experienced significant increases in surface velocity, surface thinning, and grounding line retreat since the 1990's (Rignot et al., 2002, 2014; Pritchard et al., 2009)." *to* "Glaciers of the Amundsen Sea Embayment (ASE) in West Antarctica have experienced significant increases in surface velocity, dynamic thinning, and grounding line retreat since the 1990's (Rignot et al., 2002, 2014; Pritchard et al., 2009; Flament and Rémy, 2012)."

10. *Modified* "The internal change in ice dynamics of these glaciers likely stems from the advection of warm Circumpolar Deep Water, which enhanced ocean melt causing thinning of the buttressing peripheral ice shelves (Jacobs et al., 2011)." *to* "The dynamical change of these glaciers likely stems from the advection of warm Circumpolar Deep Water, which enhanced ocean-driven melt causing thinning of the buttressing peripheral ice shelves (Jacobs et al., 2011)."

11. *Added* "We provide a set of co-registered laser altimetry datasets for evaluating estimates from satellite altimetry, photogrammetry and model outputs."

12. *Deleted* “(WFF)”

13. *Deleted* “(GSFC)”

14. *Modified* “The spatial coverage of each instrument in Antarctica over Pre-IceBridge and NASA Operation IceBridge campaigns is shown in Figure 1.” *to* “The spatial coverages of each instrument in Antarctica for the campaigns prior to and during NASA Operation IceBridge are shown in Figure 1.”

15. *Modified* “The ellipsoid heights for each instrument were converted into geoid heights using coefficients from the GGM05 gravity model provided by the Center for Space Research (Ries et al., 2016).” *to* “In order to track changes in ice shelf freeboard, the ellipsoid heights for each instrument were converted to be in reference to the GGM05 geoid using gravity model coefficients provided by the Center for Space Research (Ries et al., 2016).”

16. *Added* “Changes in ice shelf freeboard are converted into changes in ice thickness by assuming hydrostatic equilibrium following Fricker et al. (2001).”

17. *Added* “Uncertainties for each instrument were calculated following Sutterley et al. (2018).”

18. *Modified* “(Sutterley et al., 2018; Moholdt et al., 2014)” *to* “(Sutterley et al., 2018; Moholdt et al., 2014; Shean et al., 2018)”

19. *Added* “static”

20. *Modified* “. (Figure 2)” *to* “(Figure 2).”

21. *Added* “The elevation at each vertex point is weighted in the interpolation by the area of the triangle created by the enclosed point and the two opposing vertices (Sutterley et al., 2018).”

22. *Added* “(∼10–100 meters)”

23. *Added* “In order to minimize the possibility of co-registering measurements over ice shelves with measurements over grounded ice near the grounding zone or measurements over the ocean, sea ice floes and icebergs, we only include points that are on the ice shelf for the compared time periods using grounded ice delineations from Rignot et al. (2016) and Mouginot et al. (2017b) and ice shelf extent delineations manually digitized from Landsat imagery courtesy of the U.S. Geological Survey and MODIS imagery from Scambos et al. (2001).”

24. *Added* “For comparison, we compile elevation change measurements using an Eulerian approach with the Triangulated Irregular Networks (TINs) technique outlined in Sutterley et al. (2018) and a Lagrangian overlapping footprint approach following Slobbe et al. (2008) and Moholdt et al. (2014).”

25. *Added* “The Eulerian TINs scheme follows the methods of Pritchard et al. (2012) and Rignot et al. (2013) that used data from the NASA ICESat mission. Measurements compiled using the Eulerian TINs scheme have been corrected for ice strain effects following Moholdt et al. (2014).”

26. *Added* “The Lagrangian overlapping footprint approach uses the same fourth-order Runge-Kutta algorithm to advect the coordinates of the original elevation measurement to a predicted parcel location at a separate time.”

27. *Added* "If any measurements from the separate flight line lie within 100m of the advected point, the elevation measurement closest in Euclidean distance to the advected point is compared against the original measurement."

28. *Added* "the initial release of"

29. *Deleted* "(GSFC)"

30. *Added* "Uncertainties in tidal oscillations were estimated using constituent uncertainties from King et al. (2011)."

31. *Modified* "(Legos; Carrère and Lyard, 2003)" *to* "(Carrère and Lyard, 2003)"

32. *Added* "Regional sea levels fluctuate due to changes in ocean dynamics, ocean mass, and ocean heat content (Church et al., 2011; Armitage et al., 2018)."

33. *Deleted* "over ice-free ocean points"

34. *Modified* "(Le Traon et al., 1998; CMEMS)" *to* "(Le Traon et al., 1998)"

35. *Added* "The non-tidal sea surface anomalies are added to estimates of mean dynamic topography, which is the mean deviation of the sea surface from the Earth's geoid due to ocean circulation."

36. *Added* "The sea surface anomalies are extrapolated from the valid ice-free ocean values to the ice shelf points following Paolo et al. (2016)."

37. *Deleted* "(IMAU)"

38. *Modified* "We use 5.5km horizontal resolution outputs for the Antarctic Peninsula (XPEN055, van Wessem et al., 2016) and West Antarctica (ASE055, Lenaerts et al., 2018)." *to* "We use 5.5km horizontal resolution outputs from a 1979–2016 climate simulation of the Antarctic Peninsula (XPEN055, van Wessem et al., 2016) and a 1979–2015 climate simulation of West Antarctica (ASE055, Lenaerts et al., 2018)."

39. *Modified* "(van Wessem et al., 2016, Figure 4)" *to* "(van Wessem et al., 2016)"

40. *Added* "The higher spatial resolution topography improves the modeling of wind-driven downstream effects over ice shelves (Datta et al., 2018)."

41. *Modified* "The absolute precision of the RACMO2.3p2 model outputs has been estimated using field data, such as ice cores and surface stake measurements (van de Berg et al., 2006)." *to* "The absolute precision of the RACMO2.3p2 model outputs has been estimated using Operation IceBridge snow radar observations, satellite observations of surface melt, and and in-situ observations, such as ice cores and surface stake measurements, following Kuipers Munneke et al. (2017) and Lenaerts et al. (2018)."

42. *Added* "We assume a 15% uncertainty in surface mass balance and firn height change following estimates from Kuipers Munneke et al. (2017)."

43. *Added* "(M_s)"

44. *Added* "(M_b)"

45. *Added* "$(M\nabla \cdot V)$"

46. *Modified* "(Equation 1, Moholdt et al., 2014)" *to* "(Moholdt et al., 2014)"

47. *Modified* "Modified Equation 1" *to* "$\frac{dM_s}{dt} + \frac{dM_b}{dt} - M\nabla \cdot V = \frac{\rho_w \rho_{ice}}{\rho_w - \rho_{ice}} \left(\frac{Dh}{Dt} - \frac{\partial h_{oc}}{\partial t} - \frac{\partial h_{fc}}{\partial t} \right)$"

48. *Deleted* "inSAR-derived"

49. *Modified* "Mouginot et al. (2017a)" *to* "Rignot et al. (2017)"

50. *Modified* "smoothes" *to* "smooths"

51. *Added* "Deviations from mean ice flow were calculated using annually resolved ice velocity maps derived from synthetic aperture radar and optical imagery (Mouginot et al., 2017a)."

52. *Added* "and uncertainties"

53. *Modified* "is" *to* "are"

54. *Modified* "areas 1–8 kilometers downstream of the grounding zone" *to* "areas downstream of the 1–8 km wide grounding zones"

55. *Added* "3.1 Larsen Ice Shelves"

56. *Added* "The ice shelves draining from the Antarctic Peninsula into the Weddell Sea have undergone some significant changes over the past three decades."

57. *Added* "The Larsen-A Ice Shelf collapsed in 1995, and the Larsen-B Ice Shelf partially collapsed in 2002 (Rott et al., 2002, 2011)."

58. *Added* "The tributary glaciers once flowing into these shelves accelerated with the loss of the ice shelf abutment (Rignot et al., 2008)."

59. *Added* "Remnant"

60. *Modified* "ice shelves" *to* "Ice Shelves"

61. *Modified* "thickness change" *to* "melt"

62. *Modified* "ice shelf" *to* "Ice Shelf"

63. *Modified* "thickness change" *to* "melt"

64. *Modified* "ice shelf" *to* "Ice Shelf"

65. *Added* "Any uncertainties in reconstructing the regional SMB will significantly impact the resultant basal melt rate estimate."

66. *Added* "We compare our airborne laser altimetry estimate of basal melt rates with a long-term record derived from radar altimetry (Adusumilli et al., 2018)."

67. *Added* "We find that the radar-derived estimate is comparable with the laser-derived estimate within uncertainties for most points outside of the grounding zone (Figure 7)."

68. *Added* "3.2 Wilkins Ice Shelf"

69. *Deleted* “Figure 7 shows the change in ice thickness (a-b) and estimated basal thickness change rates (c-d) of the Wilkins ice shelf for two 3-year periods from 2008–2011 and 2011–2014.”

70. *Modified* “ice shelf” *to* “Ice Shelf”

71. *Modified* “ice shelf” *to* “Ice Shelf”

72. *Deleted* “The delineations were manually digitized as the ice shelf is heavily crevassed in regions near the ice edge and the bay is often filled with ice mélange (Figure 7).”

73. *Added* “Figure 8 shows the change in ice thickness (a-b) and estimated basal melt rates (c-d) of the Wilkins Ice Shelf for two 3-year periods from 2008–2011 and 2011–2014.”

74. *Modified* “ice shelf” *to* “Ice Shelf”

75. *Modified* “thickness change” *to* “melt”

76. *Added* “3.3 Pine Island Ice Shelf”

77. *Added* “The Pine Island Ice Shelf abuts one of the most rapidly changing glaciers in Antarctica (Pritchard et al., 2009; Flament and Rémy, 2012).”

78. *Modified* “thickness change” *to* “melt”

79. *Modified* “ice shelf” *to* “Ice Shelf”

80. *Added* “In this area that was previously grounded, the average estimated basal melt rates from the flight lines were 70$\pm$20 m/yr over 2009–2011 and 54$\pm$15 m/yr over 2011–2015.”

81. *Modified* “(Rignot, 2002)” *to* “(Rignot, 2002; Shean et al., 2018)”

82. *Added* “However, some of the changes in basal melt rate over the period could be due to large regional interannual-to-decadal variability (Dutrieux et al., 2014; Paolo et al., 2015; Jenkins et al., 2018).”

83. *Added* “3.4 Dotson and Crosson Ice Shelves”

84. *Deleted* “Ice thickness change rates (a-b) and estimated basal thickness change rates (c-d) of the Dotson and Crosson ice shelves for two periods from 2002–2010 and 2010–2015 are shown in Figure 9.”

85. *Modified* “ice shelves” *to* “Ice Shelves”

86. *Modified* “ice shelf” *to* “Ice Shelf”

87. *Added* “Ice thickness change rates (a-b) and estimated basal melt rates (c-d) of the Dotson and Crosson Ice Shelves are shown in Figure 10 for two periods, 2002–2010 and 2010–2015.”

88. *Modified* “thinning rates” *to* “melt rates”

89. *Modified* “thickness” *to* “elevation”

90. *Modified* “(Moholdt et al., 2014, Figure 10)” *to* “(Moholdt et al., 2014, Figure 4)”

91. *Modified* “(Moholdt et al., 2014)” *to* “(Moholdt et al., 2014; Shean et al., 2018)”

92. *Deleted* “Our Eulerian approach uses the same Triangulated Irregular Networks (TINs) technique but keeps the point measurement locations static.”

93. *Deleted* “The Eulerian scheme is similar to the methods of Pritchard et al. (2012) and Rignot et al. (2013) that used ICESat data and required spatial smoothing of the elevation change rates to filter out the effects of advected surface roughness.”

94. *Modified* “Moholdt et al. (2014) showed a similar improvement when comparing Lagrangian and Eulerian-derived estimates in bottom melt for the Ross and Filchner-Ronne ice shelves.” *to* “Moholdt et al. (2014) showed similar improvements in estimating basal melt rates between Eulerian and Lagrangian processing methods for the Ross and Filchner-Ronne Ice Shelves.”

95. *Modified* “ICESat data” *to* “data from the ICESat mission”

96. *Modified* “Lagrangian tracking of airborne data requires 1) a sufficiently wide scanning swath, 2) accurate flow-line flight planning or 3) dense grid measurements.” *to* “Lagrangian tracking of airborne data requires 1) accurate flow-line flight planning, 2) a sufficiently wide scanning swath, or 3) dense grid measurements.”

97. *Added* “Flight lines along-flow need to be accurately planned to ensure upstream measurements can be paired with future downstream measurements.”

98. *Modified* “ice shelf” *to* “Ice Shelf”

99. *Modified* “ice shelves” *to* “Ice Shelves”

100. *Modified* “the airborne data are” *to* “repeated airborne data is”

101. *Modified* “individual” *to* “singular”

102. *Added* “due to the spatial variability of ice thickness change”

103. *Modified* “Satellite altimetry measurements from ICESat-2 (Markus et al., 2017) should help rectify the data limitation problem by providing dense point clouds which could be combined with photogrammetric digital elevation models (DEMs) to create ice shelf-wide thickness change maps.” *to* “Satellite altimetry measurements from ICESat-2 (Markus et al., 2017) should help rectify the data limitation problem by providing dense and repeated point clouds. ICESat-2 data could be combined with photogrammetric digital elevation models (DEMs) to create high-resolution ice shelf-wide thickness change maps (Berger et al., 2017; Shean et al., 2018).”

104. *Deleted* “A more comprehensive update from the ICESat results of Pritchard et al. (2012) and Rignot et al. (2013) will be possible once ICESat-2 data become available.”

105. *Added* “Combining ICESat-2 with DEMs would help improve the use of the laser altimetry data in a Lagrangian reference frame as ice parcels could be accurately tracked between separate satellite tracks.”

106. *Modified* “ice shelf” *to* “Ice Shelf”

107. *Modified* “(Hogg and Gudmundsson, 2017, Figure 5)” *to* “(Hogg and Gudmundsson, 2017, Figure 6)”

108. *Modified* “velocity time series” *to* “time-variable velocity maps”

109. *Added* "(Fahnestock et al., 2016; Gardner et al., 2018; Mouginot et al., 2017a)"

110. *Added* "Improvements in ice thickness and ice velocity estimates will also greatly improve estimates of flux divergence and as a consequence estimates of basal melt rates calculated using mass conservation (Berger et al., 2017; Adusumilli et al., 2018)."

111. *Deleted* "Our study provides a validation dataset for floating ice shelves using high-resolution airborne laser altimetry data."

112. *Added* "Idealistically, the laser altimeter will detect the snow surface and the radar altimeter will detect the snow-ice interface."

113. *Added* "Because laser altimeters ideally detect the snow surface, an estimate of the total column snow/firn height change is needed to calculate the ice shelf freeboard change (Pritchard et al., 2012)."

114. *Modified* "Variations in the dielectric properties of the snow due to variable temperatures and snow grain sizes can affect the radar penetration depth (Rémy and Parouty, 2009)." *to* "For radar altimeters, the radar penetration depth is affected by variations in the dielectric properties of the surface layer due to variations in temperature, snow grain size, snow density and moisture content (Partington et al., 1989; Rémy and Parouty, 2009)."

115. *Added* "Due to the variations in penetration depth, estimates of the firn height change below the detected surface are necessary in order to calculate the freeboard change."

116. *Added* "Our study provides a validation dataset for floating ice shelves using high-resolution airborne laser altimetry data (Figure 7)."

117. *Deleted* ", the two methods most applicable to airborne data,"

118. *Deleted* "Figure 4 (previous)"

119. *Replaced* "Figure 4" *with* "Figure 10 (previous)"

120. *Replaced* "Figure 5" *with* "Figure 6 (previous)"

121. *Replaced* "Figure 6" *with* "Figure 5 (previous)"

122. *Added* "Figure 7"

123. *Replaced* "Figure 8" *with* "Figure 7 (previous)"

124. *Replaced* "Figure 9" *with* "Figure 8 (previous)"

125. *Replaced* "Figure 10" *with* "Figure 9 (previous)"

References

Adusumilli, S., Fricker, H. A., Siegfried, M. R., Padman, L., Paolo, F. S., and Ligtenberg, S. R. M.: Variable Basal Melt Rates of Antarctic Peninsula Ice Shelves, 1994–2016, Geophysical Research Letters, 45, 4086–4095, doi: 10.1002/2017GL076652, URL https://doi.org/10.1002/2017GL076652, 2018.

Armitage, T. W. K., Kwok, R., Thompson, A. F., and Cunningham, G.: Dynamic Topography and Sea Level Anomalies of the Southern Ocean: Variability and Teleconnections, Journal of Geophysical Research: Oceans, 123, 613–630, doi: 10.1002/2017JC013534, URL https://doi.org/10.1002/2017JC013534, 2018.

Berger, S., Drews, R., Helm, V., Sun, S., and Pattyn, F.: Detecting high spatial variability of ice shelf basal mass balance, Roi Baudouin Ice Shelf, Antarctica, The Cryosphere, 11, 2675–2690, doi: 10.5194/tc-11-2675-2017, URL https://www.the-cryosphere.net/11/2675/2017/, 2017.

Berthier, E., Scambos, T. A., and Shuman, C. A.: Mass loss of Larsen B tributary glaciers (Antarctic Peninsula) unabated since 2002, Geophysical Research Letters, 39, doi: 10.1029/2012GL051755, URL http://doi.wiley.com/10.1029/2012GL051755, l13501, 2012.

Brunt, K. M., Fricker, H. A., Padman, L., Scambos, T. A., and O'Neel, S.: Mapping the grounding zone of the Ross Ice Shelf, Antarctica, using ICESat laser altimetry, Annals of Glaciology, 51, 71–79, doi: 10.3189/172756410791392790, URL https://doi.org/10.3189/172756410791392790, 2010.

Brunt, K. M., Fricker, H. A., and Padman, L.: Analysis of ice plains of the Filchner–Ronne Ice Shelf, Antarctica, using ICESat laser altimetry, Journal of Glaciology, 57, 965–975, doi: 10.3189/002214311798043753, URL http://dx.doi.org/10.3189/002214311798043753, 2011.

Carrère, L. and Lyard, F.: Modeling the barotropic response of the global ocean to atmospheric wind and pressure forcing - comparisons with observations, Geophysical Research Letters, 30, doi: 10.1029/2002GL016473, URL http://dx.doi.org/10.1029/2002GL016473, 1275, 2003.

Church, J. A., White, N. J., Konikow, L. F., Domingues, C. M., Cogley, J. G., Rignot, E. J., Gregory, J. M., van den Broeke, M. R., Monaghan, A. J., and Velicogna, I.: Revisiting the Earth's sea-level and energy budgets from 1961 to 2008, Geophysical Research Letters, 38, doi: 10.1029/2011GL048794, URL http://dx.doi.org/10.1029/2011GL048794, l18601, 2011.

CMEMS: Ssalto/Duacs altimeter products were produced and distributed by the Copernicus Marine and Environment Monitoring Service (CMEMS), URL http://www.marine.copernicus.eu, 2017.

Datta, R. T., Tedesco, M., Agosta, C., Fettweis, X., Kuipers Munneke, P., and van den Broeke, M. R.: Melting over the northeast Antarctic Peninsula (1999–2009): evaluation of a, The Cryosphere, 12, 2901–2922, doi: 10.5194/tc-12-2901-2018, URL https://www.the-cryosphere.net/12/2901/2018/, 2018.

Dutrieux, P., De Rydt, J., Jenkins, A., Holland, P. R., Ha, H. K., Lee, S. H., Steig, E. J., Ding, Q., Abrahamsen, E., and Schröder, M.: Strong Sensitivity of Pine Island Ice-Shelf Melting to Climatic Variability, Science, 343, 174–178, doi: 10.1126/science.1244341, URL http://science.sciencemag.org/content/343/6167/174, 2014.

Fahnestock, M., Scambos, T., Moon, T., Gardner, A., Haran, T., and Klinger, M.: Rapid large-area mapping of ice flow using Landsat 8, Remote Sensing of Environment, 185, 84–94, doi: 10.1016/j.rse.2015.11.023, URL http://dx.doi.org/10.1016/j.rse.2015.11.023, 2016.

Flament, T. and Rémy, F.: Dynamic thinning of Antarctic glaciers from along-track repeat radar altimetry, Journal of Glaciology, 58, 830–840, doi: 10.3189/2012JoG11J118, URL http://dx.doi.org/10.3189/2012JoG11J118, 2012.

Fretwell, P., Pritchard, H. D., Vaughan, D. G., Bamber, J. L., Barrand, N. E., Bell, R. E., Bianchi, C., Bingham, R. G., Blankenship, D. D., Casassa, G., Catania, G. A., Callens, D., Conway, H., Cook, A. J., Corr, H. F. J., Damaske, D., Damm, V., Ferraccioli, F., Forsberg, R., Fujita, S., Gim, Y., Gogineni, S. P., Griggs, J. A., Hindmarsh, R. C. A., Holmlund, P., Holt, J. W., Jacobel, R. W., Jenkins, A., Jokat, W., Jordan, T. A., King, E. C., Kohler, J., Krabill, W. B., Riger-Kusk, M., Langley, K. A., Leitchenkov, G., Leuschen, C., Luyendyk, B. P., Matsuoka, K., Mouginot, J., Nitsche, F. O., Nogi, Y., Nost, O. A., Popov, S. V., Rignot, E. J., Rippin, D. M., Rivera, A., Roberts, J. L., Ross, N., Siegert, M. J., Smith, A. M., Steinhage, D., Studinger, M., Sun, B., Tinto, B. K., Welch, B. C., Wilson, D., Young, D. A., Xiangbin, C., and Zirizzotti, A.: Bedmap2: improved ice bed, surface and thickness datasets for Antarctica, The Cryosphere, 7, 375–393, doi: 10.5194/tc-7-375-2013, URL http://www.the-cryosphere.net/7/375/2013/, 2013.

Fricker, H. A., Popov, S., Allison, I., and Young, N.: Distribution of marine ice beneath the Amery Ice Shelf, Geophysical Research Letters, 28, 2241–2244, doi: 10.1029/2000GL012461, URL http://dx.doi.org/10.1029/2000GL012461, 2001.

Gagliardini, O., Durand, G., Zwinger, T., Hindmarsh, R. C. A., and Le Meur, E.: Coupling of ice-shelf melting and buttressing is a key process in ice-sheets dynamics, Geophysical Research Letters, 37, n/a–n/a, doi: 10.1029/2010GL043334, URL https://doi.org/10.1029/2010GL043334, 2010.

Gardner, A. S., Moholdt, G., Scambos, T., Fahnstock, M., Ligtenberg, S., van den Broeke, M., and Nilsson, J.: Increased West Antarctic and unchanged East Antarctic ice discharge over the last 7 years, The Cryosphere, 12, 521–547, doi: 10.5194/tc-12-521-2018, URL https://www.the-cryosphere.net/12/521/2018/, 2018.

Hogg, A. E. and Gudmundsson, G. H.: Impacts of the Larsen-C Ice Shelf calving event, Nature Climate Change, 7, 540, doi: 10.1038/nclimate3359, URL http://dx.doi.org/10.1038/nclimate3359, 2017.

Jacobs, S. S., Jenkins, A., Giulivi, C. F., and Dutrieux, P.: Stronger ocean circulation and increased melting under Pine Island Glacier ice shelf, Nature Geoscience, 4, 519–523, doi: 10.1038/ngeo1188, URL http://dx.doi.org/10.1038/ngeo1188, 2011.

Jenkins, A., Shoosmith, D., Dutrieux, P., Jacobs, S., Kim, T. W., Lee, S. H., Ha, H. K., and Stammerjohn, S.: West Antarctic Ice Sheet retreat in the Amundsen Sea driven by decadal oceanic variability, Nature Geoscience, 11, 733–738, doi: 10.1038/s41561-018-0207-4, URL https://doi.org/10.1038/s41561-018-0207-4, 2018.

Khazendar, A., Rignot, E. J., Schroeder, D. M., Seroussi, H., Schodlok, M. P., Scheuchl, B., Mouginot, J., Sutterley, T. C., and Velicogna, I.: Rapid submarine ice melting in the grounding zones of ice shelves in West Antarctica, Nature Communications, 7, 13 243, doi: 10.1038/ncomms13243, URL http://dx.doi.org/10.1038/ncomms13243, 2016.

King, M. A., Padman, L., Nicholls, K., Clarke, P. J., Gudmundsson, G., Kulessa, B., and Shepherd, A.: Ocean tides in the Weddell Sea: New observations on the Filchner-Ronne and Larsen C ice shelves and model validation, Journal of Geophysical Research: Oceans, 116, doi: 10.1029/2011JC006949, URL http://dx.doi.org/10.1029/2011JC006949, c06006, 2011.

Kuipers Munneke, P., McGrath, D., Medley, B., Luckman, A., Bevan, S., Kulessa, B., Jansen, D., Booth, A., Smeets, P., Hubbard, B., Ashmore, D., Van den Broeke, M., Sevestre, H., Steffen, K., Shepherd, A., and Gourmelen, N.: Observationally constrained surface mass balance of Larsen C ice shelf, Antarctica, The Cryosphere, 11, 2411–2426, doi: 10.5194/tc-11-2411-2017, URL https://www.the-cryosphere.net/11/2411/2017/, 2017.

Le Traon, P. Y., Nadal, F., and Ducet, N.: An Improved Mapping Method of Multisatellite Altimeter Data, Journal of Atmospheric and Oceanic Technology, 15, 522–534, doi: 10.1175/1520-0426(1998)015⟨0522:AIMMOM⟩2.0.CO;2, URL http://dx.doi.org/10.1175/1520-0426(1998)015<0522:aimmom>2.0.co;2, 1998.

Legos: Dynamic atmospheric Corrections are produced by CLS Space Oceanography Division using the Mog2D model from Legos distributed by Aviso, with support from CNES, URL https://www.aviso.altimetry.fr/en/data/products/auxiliary-products/atmospheric-corrections.html, 2017.

Lenaerts, J. T. M., Ligtenberg, S. R. M., Medley, B., Van de Berg, W. J., Konrad, H., Nicolas, J. P., Van Wessem, J. M., Trusel, L. D., Mulvaney, R., Tuckwell, R. J., Hogg, A. E., and Thomas, E. R.: Climate and surface mass balance of coastal West Antarctica resolved by regional climate modelling, Annals of Glaciology, 59, 29–41, doi: 10.1017/aog.2017.42, URL https://doi.org/10.1017/aog.2017.42, 2018.

Lilien, D. A., Joughin, I., Smith, B., and Shean, D. E.: Changes in flow of Crosson and Dotson ice shelves, West Antarctica, in, The Cryosphere, 12, 1415–1431, doi: 10.5194/tc-12-1415-2018, URL https://www.the-cryosphere.net/12/1415/2018/, 2018.

LPDAAC: NASA Landsat Program, NASA EOSDIS Land Processes Distributed Active Archive Center (LP DAAC), USGS/Earth Resources Observation and Science (EROS) Center, Sioux Falls, South Dakota, URL https://lpdaac.usgs.gov/, 2017.

Markus, T., Neumann, T., Martino, A., Abdalati, W., Brunt, K., Csatho, B., Farrell, S., Fricker, H., Gardner, A., Harding, D., Jasinski, M., Kwok, R., Magruder, L., Lubin, D., Luthcke, S., Morison, J., Nelson, R., Neuenschwander, A., Palm, S., Popescu, S., Shum, C., Schutz, B. E., Smith, B., Yang, Y., and Zwally, J.: The Ice, Cloud, and land Elevation Satellite-2 (ICESat-2): Science requirements, concept, and implementation, Remote Sensing of Environment, 190, 260–273, doi: 10.1016/j.rse.2016.12.029, URL https://doi.org/10.1016/j.rse.2016.12.029, 2017.

Moholdt, G., Padman, L., and Fricker, H. A.: Basal mass budget of Ross and Filchner-Ronne ice shelves, Antarctica, derived from Lagrangian analysis of ICESat altimetry, Journal of Geophysical Research: Earth Surface, 119, 2361–2380, doi: 10.1002/2014JF003171, URL http://dx.doi.org/10.1002/2014JF003171, 2014JF003171, 2014.

Mouginot, J., Rignot, E. J., and Scheuchl, B.: Sustained increase in ice discharge from the Amundsen Sea Embayment, West Antarctica, from 1973 to 2013, Geophysical Research Letters, 41, 1576–1584, doi: 10.1002/2013GL059069, URL http://dx.doi.org/10.1002/2013GL059069, 2014.

Mouginot, J., Rignot, E., Scheuchl, B., and Millan, R.: Comprehensive Annual Ice Sheet Velocity Mapping Using Landsat-8, Sentinel-1, and RADARSAT-2 Data, Remote Sensing, 9, doi: 10.3390/rs9040364, URL http://www.mdpi.com/2072-4292/9/4/364, 364, 2017a.

Mouginot, J., Scheuchl, B., and Rignot, E.: MEaSUREs Antarctic Boundaries for IPY 2007–2009 from Satellite Radar, NASA National Snow and Ice Data Center Distributed Active Archive Center, Boulder, Colorado USA, doi: 10.5067/AXE4121732AD, URL http://dx.doi.org/10.5067/AXE4121732AD, version 2, 2017b.

Paolo, F. S., Fricker, H. A., and Padman, L.: Volume loss from Antarctic ice shelves is accelerating, Science, 348, 327–331, doi: 10.1126/science.aaa0940, URL http://science.sciencemag.org/content/348/6232/327.abstract, 2015.

Paolo, F. S., Fricker, H. A., and Padman, L.: Constructing improved decadal records of Antarctic ice shelf height change from multiple satellite radar altimeters, Remote Sensing of Environment, 177, 192–205, doi: 10.1016/j.rse.2016.01.026, URL http://linkinghub.elsevier.com/retrieve/pii/S0034425716300268, 2016.

Partington, K. C., Ridley, J. K., Rapley, C. G., and Zwally, H. J.: Observations of the Surface Properties of the Ice Sheets by Satellite Radar Altimetry, Journal of Glaciology, 35, 267–275, doi: 10.3189/S0022143000004603, URL https://doi.org/10.3189/S0022143000004603, 1989.

Pritchard, H. D., Arthern, R. J., Vaughan, D. G., and Edwards, L. A.: Extensive dynamic thinning on the margins of the Greenland and Antarctic ice sheets, Nature, 461, 971–975, doi: 10.1038/nature08471, URL http://www.nature.com/nature/journal/vaop/ncurrent/full/nature08471.html), 2009.

Pritchard, H. D., Ligtenberg, S. R. M., Fricker, H. A., Vaughan, D. G., van den Broeke, M. R., and Padman, L.: Antarctic ice-sheet loss driven by basal melting of ice shelves, Nature, 484, 502–505, doi: 10.1038/nature10968, URL http://www.nature.com/doifinder/10.1038/nature10968, 2012.

Rémy, F. and Parouty, S.: Antarctic Ice Sheet and Radar Altimetry: A Review, Remote Sensing, 1, 1212–1239, doi: 10.3390/rs1041212, URL http://www.mdpi.com/2072-4292/1/4/1212/, 2009.

Ries, J., Bettadpur, S., Eanes, R., Kang, Z., Ko, U., McCullough, C., Nagel, P., Pie, N., Poole, S., Richter, T., Save, H., and Tapley, B.: The Development and Evaluation of the Global Gravity Model GGM05, Tech. Rep. CSR-16-02, UTCSR, Austin, Texas, doi: 10.5880/icgem.2016.002, URL ftp://ftp.csr.utexas.edu/pub/grace/GGM05/CSR-16-02.pdf, 2016.

Rignot, E.: Ice-shelf changes in Pine Island Bay, Antarctica, 1947–2000, Journal of Glaciology, 48, 247–256, doi: 10.3189/172756502781831386, URL http://dx.doi.org/10.3189/172756502781831386, 2002.

Rignot, E. J. and Jacobs, S.: Rapid Bottom Melting Widespread near Antarctic Ice Sheet Grounding Lines, Science, 296, 2020–2023, doi: 10.1126/science.1070942, URL http://www.sciencemag.org/cgi/doi/10.1126/science.1070942, 2002.

Rignot, E. J., Vaughan, D. G., Schmeltz, M., Dupont, T., and MacAyeal, D. R.: Acceleration of Pine Island and Thwaites Glaciers, West Antarctica, Annals of Glaciology, 34, 189–194, doi: 10.3189/172756402781817950, URL http://dx.doi.org/10.3189/172756402781817950, 2002.

Rignot, E. J., Casassa, G., Gogineni, S. P., Krabill, W. B., Rivera, A., and Thomas, R. H.: Accelerated ice discharge from the Antarctic Peninsula following the collapse of Larsen B ice shelf, Geophysical Research Letters, 31, doi: 10.1029/2004GL020697, URL http://dx.doi.org/10.1029/2004GL020697, l18401, 2004.

Rignot, E. J., Bamber, J. L., van den Broeke, M. R., Davis, C. H., Li, Y., van de Berg, W. J., and van Meijgaard, E.: Recent Antarctic ice mass loss from radar interferometry and regional climate modelling, Nature Geoscience, 1, 106–110, doi: 10.1038/ngeo102, URL http://www.nature.com/ngeo/journal/v1/n2/abs/ngeo102.html, 2008.

Rignot, E. J., Jacobs, S., Mouginot, J., and Scheuchl, B.: Ice-Shelf Melting Around Antarctica, Science, 341, 266–270, doi: 10.1126/science.1235798, URL http://science.sciencemag.org/content/341/6143/266, 2013.

Rignot, E. J., Mouginot, J., Morlighem, M., Seroussi, H., and Scheuchl, B.: Widespread, rapid grounding line retreat of Pine Island, Thwaites, Smith, and Kohler glaciers, West Antarctica, from 1992 to 2011, Geophysical Research Letters, 41, 3502–3509, doi: 10.1002/2014GL060140, URL http://dx.doi.org/10.1002/2014GL060140, 2014.

Rignot, E. J., Mouginot, J., and Scheuchl, B.: MEaSUREs Antarctic Grounding Line from Differential Satellite Radar Interferometry, NASA National Snow and Ice Data Center Distributed Active Archive Center, Boulder, Colorado USA, doi: 10.5067/IKBWW4RYHF1Q, URL http://dx.doi.org/10.5067/IKBWW4RYHF1Q, version 2, 2016.

Rignot, E. J., Mouginot, J., and Scheuchl, B.: MEaSUREs InSAR-Based Antarctica Ice Velocity Map, NASA National Snow and Ice Data Center Distributed Active Archive Center, Boulder, Colorado USA, doi: 10.5067/D7GK8F5J8M8R, URL http://dx.doi.org/10.5067/D7GK8F5J8M8R, version 2, 2017.

Rott, H., Rack, W., Skvarca, P., and De Angelis, H.: Northern Larsen Ice Shelf, Antarctica: further retreat after collapse, Annals of Glaciology, 34, 277–282, doi: 10.3189/172756402781817716, URL https://doi.org/10.3189/172756402781817716, 2002.

Rott, H., Müller, F., Nagler, T., and Floricioiu, D.: The imbalance of glaciers after disintegration of Larsen-B ice shelf, Antarctic Peninsula, The Cryosphere, 5, 125–134, doi: 10.5194/tc-5-125-2011, URL http://www.the-cryosphere.net/5/125/2011/, 2011.

Scambos, T., Raup, B. H., and Bohlander, J.: Images of Antarctic Ice Shelves, NASA National Snow and Ice Data Center Distributed Active Archive Center, Boulder, Colorado USA, doi: 10.7265/N5NC5Z4N, URL http://dx.doi.org/10.7265/N5NC5Z4N, version 1, 2001.

Shean, D. E., Joughin, I. R., Dutrieux, P., Smith, B. E., and Berthier, E.: Ice shelf basal melt rates from a high-resolution DEM record for Pine Island Glacier, Antarctica, The Cryosphere Discussions, 2018, 1–39, doi: 10.5194/tc-2018-209, URL https://www.the-cryosphere-discuss.net/tc-2018-209/, 2018.

Slobbe, D. C., Lindenbergh, R. C., and Ditmar, P.: Estimation of volume change rates of Greenland's ice sheet from ICESat data using overlapping footprints, Remote Sensing of Environment, 112, 4204–4213, doi: 10.1016/j.rse.2008.07.004, URL http://www.sciencedirect.com/science/article/pii/S0034425708002277, 2008.

Sutterley, T. C., Velicogna, I., Rignot, E. J., Mouginot, J., Flament, T., van den Broeke, M. R., van Wessem, J. M., and Reijmer, C. H.: Mass loss of the Amundsen Sea Embayment of West Antarctica from four independent techniques, Geophysical Research Letters, 41, 8421–8428, doi: 10.1002/2014GL061940, URL http://doi.wiley.com/10.1002/2014GL061940, 2014GL061940, 2014.

Sutterley, T. C., Velicogna, I., Fettweis, X., Rignot, E., Noël, B., and van den Broeke, M.: Evaluation of Reconstructions of Snow/Ice Melt in Greenland by Regional Atmospheric Climate Models Using Laser Altimetry Data, Geophysical Research Letters, 45, 8324–8333, doi: 10.1029/2018GL078645, URL https://doi.org/10.1029/2018GL078645, 2018.

van de Berg, W. J., van den Broeke, M. R., Reijmer, C. H., and van Meijgaard, E.: Reassessment of the Antarctic surface mass balance using calibrated output of a regional atmospheric climate model, Journal of Geophysical Research: Atmospheres, 111, doi: 10.1029/2005JD006495, URL http://dx.doi.org/10.1029/2005JD006495, d11104, 2006.

van Wessem, J. M., Ligtenberg, S. R. M., Reijmer, C. H., van de Berg, W. J., van den Broeke, M. R., Barrand, N. E., Thomas, E. R., Turner, J., Wuite, J., Scambos, T. A., and van Meijgaard, E.: The modelled surface mass balance of the Antarctic Peninsula at 5.5 km horizontal resolution, The Cryosphere, 10, 271–285, doi: 10.5194/tc-10-271-2016, URL http://www.the-cryosphere.net/10/271/2016/, 2016.

Walker, D. P., Brandon, M. A., Jenkins, A., Allen, J. T., Dowdeswell, J. A., and Evans, J.: Oceanic heat transport onto the Amundsen Sea shelf through a submarine glacial trough, Geophysical Research Letters, 34, n/a–n/a, doi: 10.1029/2006GL028154, URL https://doi.org/10.1029/2006GL028154, 2007.

Antarctic Ice Shelf Thickness Change from Multi-Mission Lidar Mapping

Tyler C. Sutterley[1], Thorsten Markus[1], Thomas A. Neumann[1], Michiel van den Broeke[2], J. Melchior van Wessem[2], and Stefan R. M. Ligtenberg[2]

[1]NASA Goddard Space Flight Center, Greenbelt, MD 20771

[2]Institute for Marine and Atmospheric Research, Utrecht University, Utrecht, The Netherlands

Correspondence: Tyler C. Sutterley (tyler.c.sutterley@nasa.gov)

Abstract.

We calculate rates of ice thickness change and bottom melt for ice shelves in West Antarctica and the Antarctic Peninsula from a combination of elevation measurements from Operation IceBridge corrected for oceanic and surface processes, surface velocity measurements from synthetic aperture radar, and high-resolution outputs from regional climate models. ~~We calculate~~ The ice thickness change rates are calculated in a Lagrangian reference frame to reduce the effects from advection of sharp vertical features, such as cracks and crevasses, ~~which~~ that can saturate Eulerian-derived estimates. We use our method over different ice shelves in Antarctica, which vary in terms of ~~the processes that drive their change, their sizeand their repeat coverage but are all susceptible to short-term changesin ice thickness.~~ size, repeat coverage from airborne altimetry and dominant processes governing their recent changes. We find that ice thickness variations of the Larsen-C ~~ice shelf~~ Ice Shelf are due to the flux divergence of the shelf with firn and surface processes controlling short-term variability over our observation period. The Wilkins ~~ice shelf~~ Ice Shelf is sensitive to short time-scale coastal and upper-ocean processes, and basal melt is the dominate contributor to the ice thickness change over the period. At ~~The Pine Island ice shelf~~ the Pine Island Ice Shelf in the critical region near in the grounding zone, we find that ice shelf thinning rates exceed 40 m/yr ~~. The thickness change is~~ with the change dominated by strong submarine ~~thinning~~melting. Regions near the grounding zones of the Dotson and Crosson ~~ice shelves~~ Ice Shelves are thinning at rates greater than 40 m/yr, also due to intense basal melt. Operation IceBridge provides a validation dataset for floating ice shelves at moderately high resolution when co-registered using Lagrangian methods.

1 Introduction

Most of the drainage from the Antarctic ice sheet is through its peripheral ice shelves, floating extensions of the land ice that cover 75% of the Antarctic coastline and represent 10% of the total ice covered area (Cuffey and Paterson, 2010; Rignot et al., 2013). Floating ice shelves exert control on the grounded ice sheet's overall stability by buttressing the flow of the glaciers upstream (Dupont and Alley, 2005; Rignot et al., 2013). The thinning of Antarctic ice shelves reduces their ability to buttress the glaciers that flow into them and makes the shelves more susceptible to fracture and overall collapse (Shepherd et al., 2003; Fricker and Padman, 2012). Ice shelves gain mass by the advection of ice from the land, the accumulation of snow at the surface, and the freezing of seawater at the ice shelf base (Thomas, 1979). They lose mass through runoff, wind scour and sublimation at the surface of the shelf, melting at the base of the shelf and through calving (Thomas, 1979).

Currently, several ice shelves across Antarctica are losing volume, which has led to the acceleration and intensified discharge of inland ice (Pritchard et al., 2012; Depoorter et al., 2013; Paolo et al., 2016). ~~After the 2002~~ In 2003, a year after the collapse of the ~~Larsen B ice shelf~~Larsen-B Ice Shelf, some tributary glaciers draining into the Weddell Sea from the Antarctic Peninsula ~~accelerated 2 to 8 times their previous flow rates , and~~ flowed at rates 2–8 times their 1996 flow rates (Rignot et al., 2004). These glaciers continued flowing at the accelerated rates years after the collapse ~~(Rignot et al., 2004, 2008; Berthier et al., 2012)~~ (Rignot et al., 2008; Berthier et al., 2012). Glaciers of the Amundsen Sea Embayment (ASE) in West Antarctica have experienced significant increases in surface velocity, ~~surface~~ dynamic thinning, and grounding line retreat since the 1990's ~~(Rignot et al., 2002, 2014; Pritchard et al., 2009).~~ (Rignot et al., 2002, 2014; Pritchard et al., 2009; Flament and Rémy, 2012). ~~The internal change in ice dynamics~~ The dynamical change of these glaciers likely stems from the advection of warm Circumpolar Deep Water, which enhanced ~~ocean~~ ocean-driven melt causing thinning of the buttressing peripheral ice shelves (Jacobs et al., 2011).

Here, we compile ice shelf thickness change rates calculated using a suite of airborne altimetry datasets, which have been consistently processed and co-registered. We provide a set of co-registered laser altimetry datasets for evaluating estimates from satellite altimetry, photogrammetry and model outputs. The main objectives of this study are to (i) calculate ice shelf thickness change rates, (ii) investigate processes driving the changes in the shelf, (iii) investigate the sensitivity of spatial and temporal sampling to overall estimates and (iv) evaluate different methods of calculating elevation change rates over ice shelves. In the following sections, we discuss the co-registration method, the geophysical corrections applied, the results for a sample set of ice shelves and the overall implications of the results for ice shelf studies.

2 Materials and Methods

Our airborne lidar measurements are Level-2 Airborne Topographic Mapper (ATM Icessn) and Land, Vegetation and Ice Sensor (LVIS) datasets provided by the National Snow and Ice Data Center (NSIDC) (Thomas and Studinger, 2010; Studinger, 2014; Blair and Hofton, 2010). ATM is a conically scanning lidar which has flown in Antarctica since 2002 and was developed at the NASA Wallops Flight Facility ~~(WFF)~~ (Thomas and Studinger, 2010). LVIS is a large-swath scanning lidar which flew in Antarctica in 2009, 2010, 2011 and 2015 and was developed at NASA Goddard Space Flight Center ~~(GSFC)~~ (Blair et al., 1999; Hofton et al., 2008). For the data release available for Antarctica (LDSv1), the Level-2 LVIS data provides 3 different elevation surfaces computed from the Level-1B waveforms: the highest and lowest returning surfaces from Gaussian decomposition, and the centroidal surface (Blair and Hofton, 2010). Here, we use the lowest returning surface when the waveform resembles a single-peak gaussian and the centroid surface when the waveform is multi-peak. The spatial ~~coverage~~ coverages of each instrument in Antarctica ~~over Pre-IceBridge and~~ for the campaigns prior to and during NASA Operation IceBridge ~~campaigns is~~ are shown in Figure 1. The elevation datasets from each instrument are converted to be in reference to the 2014 solution of the International Terrestrial Reference Frame (ITRF) (Altamimi et al., 2016). ~~The~~ In order to track changes in ice shelf freeboard, the ellipsoid heights for each instrument were converted ~~into geoid heights using coefficients from~~ to be in reference to the GGM05 ~~gravity model~~ geoid using gravity model coefficients provided by the Center for Space Research (Ries et al., 2016). Changes in ice shelf freeboard are converted into changes in ice thickness by assuming hydrostatic equilibrium following Fricker et al. (2001). Uncertainties for each instrument were calculated following Sutterley et al. (2018).

2.1 Integrated analysis of altimetry

We calculate rates of elevation change by comparing a set of measured elevation values with a set of interpolated elevation values from a different time period after allowing for the advection of the ice ~~(Sutterley et al., 2018; Moholdt et al., 2014)~~ (Sutterley et al., 2018; Moholdt et al., 2014; Shean et al., 2018). Each point in a flight line is advected from its original location by integrating the Rignot et al. (2017) MEaSUREs static velocity data derived from synthetic aperture radar (SAR) using a fourth-order Runge-Kutta algorithm. For each data point in a flight line, a set of Delaunay triangles is constructed from a separate flight line using all data points within 300 meters from the final location of the advected point (Pritchard et al., 2009, 2012; Rignot et al., 2013). If the advected point lies within the confines of the Delaunay triangulation convex hull, the triangular facet housing the advected point is determined using a winding number algorithm (Sutterley et al., 2018). The new elevation value is calculated using barycentric interpolation with the elevation measurements at the three triangle vertices ~~.~~ (Figure 2). The elevation at each vertex point is weighted in the interpolation by the area of the triangle created by the enclosed point and the two opposing vertices (Sutterley et al., 2018).

Assuming that the ice shelf surfaces are not curved over the scale of the individual triangular facet (∼10–100 meters), interpolating to the advected coordinates will compensate for minor slopes in the ice shelf surface so that the elevations of equivalent parcels of ice can be compared in time (Pritchard et al., 2009). At this scale (below 100–200m), the topographic relief of uncrevassed ice is primarily due to slopes in the ice surface and a planar assumption should be largely valid (Markus et al., 2017). Rough terrain, snow drifts and low-lying clouds will contaminate the lidar elevation values for the interpolation. In order to limit the effect of contaminated points, the elevation measurements are filtered using the Robust Dispersion Estimator (RDE) algorithm described in Smith et al. (2017). In order to minimize the possibility of co-registering measurements over ice shelves with measurements over grounded ice near the grounding zone or measurements over the ocean, sea ice floes and icebergs, we only include points that are on the ice shelf for the compared time periods using grounded ice delineations from Rignot et al. (2016) and Mouginot et al. (2017b) and ice shelf extent delineations manually digitized from Landsat imagery courtesy of the U.S. Geological Survey and MODIS imagery from Scambos et al. (2001).

For comparison, we compile elevation change measurements using an Eulerian approach with the Triangulated Irregular Networks (TINs) technique outlined in Sutterley et al. (2018) and a Lagrangian overlapping footprint approach following Slobbe et al. (2008) and Moholdt et al. (2014). The Eulerian TINs scheme follows the methods of Pritchard et al. (2012) and Rignot et al. (2013) that used data from the NASA ICESat mission. Measurements compiled using the Eulerian TINs scheme have been corrected for ice strain effects following Moholdt et al. (2014). The Lagrangian overlapping footprint approach uses the same fourth-order Runge-Kutta algorithm to advect the coordinates of the original elevation measurement to a predicted parcel location at a separate time. If any measurements from the separate flight line lie within 100m of the advected point, the elevation measurement closest in Euclidean distance to the advected point is compared against the original measurement.

2.2 Geophysical Corrections

We correct the elevation measurements for geophysical processes following most of the procedures that will be used with the initial release of ICESat-2 data (Markus et al., 2017; Neumann et al., 2018). The processes are described in the following sections and represented as a schematic in Figure 3.

2.2.1 Tidal and Non-Tidal Ocean Variation

Surface elevation changes due to variations in ocean and load tides are calculated using outputs from the Circum-Antarctic Tidal Simulation (CATS2008) model (Padman et al., 2008), a high-resolution inverse model updated from Padman et al. (2002). Surface heights were predicted for the M_2, S_2, N_2, K_2, K_1, O_1, P_1, Q_1, M_f and M_m harmonic constituents and then inferred for 16 minor constituents following the *PERTH3* algorithm developed by Richard Ray at NASA Goddard Space Flight Center (GSFC) (Ray, 1999). Uncertainties in tidal oscillations were estimated using constituent uncertainties from King et al. (2011). We correct for changes in load and ocean pole tides due to changes in the Earth's rotation vector following Desai (2002) and IERS conventions (Petit and Luzum, 2010). We correct for changes in sea surface height due to changes in atmospheric pressure and wind stress using a dynamic atmosphere correction (DAC) provided by AVISO. The 6-hour DAC product combines outputs of the MOD2D-g ocean model, a 2-D ocean model forced by pressure and wind fields from ECMWF based on Lynch and Gray (1979), with an inverse barometer (IB) response (Legos; Carrère and Lyard, 2003)(Carrère and Lyard, 2003). Regional sea levels fluctuate due to changes in ocean dynamics, ocean mass, and ocean heat content (Church et al., 2011; Armitage et al., 2018). Non-tidal sea surface anomalies over ice-free ocean points are removed from the ice shelf data using multi-mission altimetry products computed by AVISO and provided by Copernicus (Le Traon et al., 1998; CMEMS). (Le Traon et al., 1998). The non-tidal sea surface anomalies are added to estimates of mean dynamic topography, which is the mean deviation of the sea surface from the Earth's geoid due to ocean circulation. The sea surface anomalies are extrapolated from the valid ice-free ocean values to the ice shelf points following Paolo et al. (2016).

2.2.2 Surface Mass Balance and Firn Compaction

After correcting for the effects of oceanic variation and advection, changes in surface height are due to a combination of accumulation, ablation and firn densification processes. To account for variations in surface elevation due to changes in surface processes, we use monthly mean surface mass balance (SMB) outputs calculated from climate simulations of the Regional Atmospheric Climate Model (RACMO2.3p2) computed by the Ice and Climate group at the Institute for Marine and Atmospheric Research of Utrecht University (IMAU) (Ligtenberg et al., 2013; van Wessem et al., 2014, 2018). We use 5.5km horizontal resolution outputs for from a 1979–2016 climate simulation of the Antarctic Peninsula (XPEN055, van Wessem et al., 2016) and a 1979–2015 climate simulation of West Antarctica (ASE055, Lenaerts et al., 2018). The high-resolution outputs better represent the surface mass balance state than outputs from the 27km ice sheet wide model, particularly in the highly complex topography of mountains and glacial valleys in the Antarctic peninsula (van Wessem et al., 2016, Figure 4). (van Wessem et al., 2016). The higher spatial resolution topography improves the modeling of wind-driven downstream effects over ice shelves (Datta et al., 2018). SMB is the quantified difference between mass inputs from the precipitation of snow and rain, and mass losses by sublimation, runoff, and wind scour (Lenaerts et al., 2012; van den Broeke et al., 2009). Runoff is the portion of total snowmelt not retained or refrozen within the ice sheet. Wind scour is the erosion and sublimation of wind-blown snow from the ice sheet surface (Das et al., 2013). The absolute precision of the RACMO2.3p2 model outputs has been estimated using field data, Operation IceBridge snow radar observations, satellite observations of surface melt, and and in-situ observations, such as ice cores and surface stake measurements(van de Berg et al., 2006), following Kuipers Munneke et al. (2017) and Lenaerts et al. (2018). To correct for variations in the firn layer thickness, we use outputs from a semi-empirical firn densification model that simulates the steady-state firn density profile (Ligtenberg et al., 2011, 2012). The firn densification model is forced with surface mass balance outputs, surface temperatures fields and near-surface wind speed fields computed by RACMO2.3p2 (Ligtenberg et al., 2011). We assume a 15% uncertainty in surface mass balance and firn height change following estimates from Kuipers Munneke et al. (2017).

2.3 Ice Shelf Bottom Melt

Changes in ice shelf mass in a Lagrangian reference frame are due to changes in surface mass balance (SMB) processes (M_s), basal melt (M_b) and the divergence of the ice shelf flow field (Equation 1, Moholdt et al., 2014). ($M\nabla\cdot V$) (Moholdt et al., 2014).

$$\frac{dM_{SMB}}{dt}\frac{dM_s}{dt} + \frac{dM_b}{dt} - M\nabla\cdot V = \frac{\rho_w\rho_{ice}}{\rho_w - \rho_{ice}}\left(\frac{dh}{dt}\frac{Dh}{Dt} - \frac{dh_{oc}}{dt}\frac{\partial h_{oc}}{\partial t} - \frac{dh_{fc}}{dt}\frac{\partial h_{fc}}{\partial t}\right) \qquad (1)$$

where ρ_w and ρ_{ice} are the densities of sea water and meteoric ice respectively, h_{oc} are ocean heights, and h_{fc} are firn-column heights. We estimate ice shelf bottom melt rates along flight lines by using mass conservation and estimates of the mass flux divergence (Rignot and Jacobs, 2002; Moholdt et al., 2014; Rignot et al., 2013). Ice flow divergence fields are calculated from inSAR-derived ice velocities from Mouginot et al. (2017a) Rignot et al. (2017) differentiated using a Savitzky-Golay filter with an 11 km half-width window (Savitzky and Golay, 1964). The Savitzky-Golay algorithm smoothes smooths the velocity field, and reduces the impact of ionospheric noise and other sources of uncertainty on the differentials. Deviations from mean ice flow were calculated using annually resolved ice velocity maps derived from synthetic aperture radar and optical imagery (Mouginot et al., 2017a). We use ice thickness data and uncertainties from Bedmap2, which is are primarily derived from Griggs and Bamber (2011) for ice shelves (Fretwell et al., 2013). The ice thickness estimates are calculated assuming hydrostatic equilibrium, which should be valid for areas 1–8 kilometers most areas downstream of the grounding zone 1–8 km wide grounding zones (Brunt et al., 2010, 2011).

3 Results

3.1 Larsen Ice Shelves

The ice shelves draining from the Antarctic Peninsula into the Weddell Sea have undergone some significant changes over the past three decades. The Larsen-A Ice Shelf collapsed in 1995, and the Larsen-B Ice Shelf partially collapsed in 2002 (Rott et al., 2002, 2011). The tributary glaciers once flowing into these shelves accelerated with the loss of the ice shelf abutment (Rignot et al., 2008). Figure 6 (a-b) shows the change in ice thickness of the Larsen-B Remnant and Larsen-C ~~ice shelves~~ Ice Shelves for two periods, 2002–2008 and 2008–2016, from Pre-IceBridge and Operation IceBridge airborne data. Figure 6 (c-d) shows the estimated basal ~~thickness change~~ melt rate of the ice shelves over the same periods. The average thickness change rate between 2008 and 2016 from the flight line data over the Larsen-C ~~ice shelf~~ Ice Shelf is –1.4±~~0.6~~ 0.9 m/yr. From 2008–2016, the strongest thinning occurs near the grounding zone, particularly for the flight lines starting near Cabinet and Mill Inlets. For a flight line starting near the Whirlwind Inlet, the ice shelf is thinning near the grounding zone at 2 m/yr (Figure 5a). Scatter in the ice thickness change rate across the flight line is typically 30–50 cm/yr, or a 4–6 cm/yr error in the measured elevation change rate (Figure 5a). Most of the thickness change along this line is due to the flux divergence of the shelf. As the basal ~~thickness change~~ melt rate is calculated via mass conservation and the observed thinning rate largely matches the flux divergence, estimates of the basal melt rate of the Larsen-C ~~ice shelf~~ Ice Shelf are highly dependent on the SMB flux estimate. Any uncertainties in reconstructing the regional SMB will significantly impact the resultant basal melt rate estimate. We compare our airborne laser altimetry estimate of basal melt rates with a long-term record derived from radar altimetry (Adusumilli et al., 2018). We find that the radar-derived estimate is comparable with the laser-derived estimate within uncertainties for most points outside of the grounding zone (Figure 7).

3.2 Wilkens Ice Shelf

~~Figure 7 shows the change in ice thickness (a-b) and estimated basal thickness change rates (c-d) of the Wilkins ice shelf for two 3-year periods from 2008–2011 and 2011–2014. The Wilkins ice shelf~~ The Wilkins Ice Shelf is fed by glaciers on Alexander Island, which is located near the west coast of the Antarctic Peninsula and is the largest of the Antarctic islands. ~~Wilkins ice shelf~~ Wilkins Ice Shelf is sensitive to short time-scale coastal and upper-ocean processes (Padman et al., 2012) and ablates largely through basal melting (Rignot et al., 2013). ~~Ice shelf extents are delineated from Landsat imagery provided courtesy of the U.S. Geological Survey (LPDAAC) and MODIS imagery provided by NSIDC (Scambos et al., 2001). The delineations were manually digitized as the ice shelf is heavily crevassed in regions near the ice edge and the bay is often filled with ice mélange .~~ Figure 8 shows the change in ice thickness (a-b) and estimated basal melt rates (c-d) of the Wilkins Ice Shelf for two 3-year periods from 2008–2011 and 2011–2014. The extent of the ice shelf reduced by over 6000 km^2 between 1990 and 2017 (Scambos et al., 2009). The partial collapse occurred once the shelf started decoupling from Charcot Island (Vaughan et al., 1993) and likely occurred due to hydro-fracturing (Scambos et al., 2009). Meltwater ponds covered areas of 300–600 km^2 in Landsat imagery in 1986 and 1990 (Vaughan et al., 1993). The ponds existed largely in the now-collapsed portions of the shelf near Rothschild Island. Average thinning rates of the Wilkins ~~ice shelf~~ Ice Shelf from the flight lines were 1.2±~~0.4~~ 0.7 m/yr from 2008–2011 and 0.7±~~0.4~~ 0.5 m/yr from 2011–2014. Average estimated basal ~~thickness change~~ melt rates from the flight lines were 2.8±~~0.3~~ 1.3 m/yr in the earlier period and 2.0±~~0.3~~ 0.9 m/yr in the latter period. Basal accretion could have occurred in some regions during the 2011–2014 period.

3.3 Pine Island Ice Shelf

The Pine Island Ice Shelf abuts one of the most rapidly changing glaciers in Antarctica (Pritchard et al., 2009; Flament and Rémy, 2012). Figure 9 shows the change in ice thickness (a-b) and estimated basal ~~thickness change~~ melt rates (c-d) of the Pine Island ~~ice shelf~~ Ice Shelf for two periods from 2009–2011 and 2011–2015. These periods were chosen to include repeat measurements from LVIS of the ice shelf near the grounding zone and to use the high-resolution outputs of RACMO2.3p2 ASE055. In the previously grounded region between the 1996 and 2011 grounding lines, the ice shelf thinning rates were 97±15 m/yr during 2009–2011 and ~~82~~81±7 m/yr during 2011–2015. In this area that was previously grounded, the average estimated basal melt rates from the flight lines were 70±20 m/yr over 2009–2011 and 54±15 m/yr over 2011–2015. Ice thickness change rates outside of the previously grounded area are significantly weaker, averaging –21±7 m/yr for 2009–2011 and –15±3 m/yr for 2011–2015. The average ice thinning rates from the flight lines were insignificantly different at 36±9 m/yr over 2009–2011 and ~~34~~35±5 m/yr over 2011–2015. Basal melt rates near the grounding zone have the highest impact on the glacial flow dynamics (Rignot and Jacobs, 2002). The difference in melt rates near the grounding zone between 2009–2011 and 2011–2015 could possibly explain some of the moderation in thinning of the grounded ice and stability in ice discharge from Pine Island Glacier after 2010 (McMillan et al., 2014; Medley et al., 2014). As shown in Figure 9c-d, the ice thickness change is dominated by strong submarine thinning, which is further evidence of the dominant oceanic controls on the ice shelf mass balance in this region ~~(Rignot, 2002).~~ (Rignot, 2002; Shean et al., 2018). However, some of the changes in basal melt rate over the period could be due to large regional interannual-to-decadal variability (Dutrieux et al., 2014; Paolo et al., 2015; Jenkins et al., 2018).

3.4 Dotson and Crosson Ice Shelves

~~Ice thickness change rates (a-b) and estimated basal thickness change rates (c-d) of the Dotson and Crosson ice shelves for two periods from 2002–2010 and 2010–2015 are shown in Figure 9.~~ The glaciers flowing into the Dotson and Crosson ~~ice shelves~~ Ice Shelves have rapidly thinned, increased in speed and experienced significant retreats of grounding line positions over the past 20 years (Mouginot et al., 2014; Scheuchl et al., 2016). Flow speeds of the Crosson ~~ice shelf~~ Ice Shelf have doubled in some regions over 1996 to 2014, while the flow speed of Dotson has remained largely steady (Lilien et al., 2018). Ice thickness change rates (a-b) and estimated basal melt rates (c-d) of the Dotson and Crosson Ice Shelves are shown in Figure 10 for two periods, 2002–2010 and 2010–2015. Regions near the grounding lines of the input glaciers are thinning rapidly for both shelves driven by strong basal melt. Basal ~~thinning rates averaged 46–71~~ melt rates averaged 45–71 m/yr near the grounding zone of Smith glacier over the two periods. Khazendar et al. (2016) documented rapid submarine ice melt and the loss of 300–490 m of floating ice between 2002 and 2009. Our work here provides independent evidence of this large-scale melt using a separate method and more years of data. We find that the ice mass wastage continued unabated between 2010 and 2015 with thinning rates over the flight lines averaging 22±1 m/yr.

4 Discussion

Using a Lagrangian reference frame produces estimates of ice shelf ~~thickness~~ elevation change with much less noise compared with a Eulerian reference frame ~~(Moholdt et al., 2014, Figure 10)~~(Moholdt et al., 2014, Figure 4). The advection of ice thickness gradients, such as that from cracks and crevasses in the ice, can saturate the Eulerian-derived estimates ~~(Moholdt et al., 2014)~~ (Moholdt et al., 2014; Shean et al., 2018). ~~Our Eulerian approach uses the same Triangulated Irregular Networks (TINs) technique but keeps the point measurement locations static. The Eulerian scheme is similar to the methods of Pritchard et al. (2012) and Rignot et al. (2013) that used ICESat data and required spatial smoothing of the elevation change rates to filter out the effects of advected surface roughness. Moholdt et al. (2014) showed a similar improvement when comparing Lagrangian and Eulerian-derived estimates in bottom melt.~~ Moholdt et al. (2014) showed similar improvements in estimating basal melt rates between Eulerian and Lagrangian processing methods for the Ross and Filchner-Ronne ~~ice shelves~~Ice Shelves. In their study, Moholdt et al. (2014) used ~~ICESat data~~ data from the ICESat mission that were integrated using an overlapping footprints scheme.

Lagrangian tracking of airborne data requires 1) accurate flow-line flight planning, 2) a sufficiently wide scanning swath, ~~2) accurate flow-line flight planning~~ or 3) dense grid measurements. Flight lines along-flow need to be accurately planned to ensure upstream measurements can be paired with future downstream measurements. With the current Operation IceBridge data at most locations, cross-flow flight lines advected outside of the swath width over multi-year repeat times. This limited our dataset to regions with flow-line measurements, such as the Larsen-C ~~ice shelf~~ Ice Shelf (Figure 6), or frequent measurements, such as the Dotson and Crosson ~~ice shelves~~ Ice Shelves (Figure 10). For most ice shelves, ~~the airborne data are~~ repeated airborne data is too sparse to extract large-scale spatial trends, particularly in the era before Operation IceBridge. Isolated crossovers can be calculated using Lagrangian tracking for some ice shelves using along-flow and cross-flow measurements from separate years. However, these ~~individual~~ singular crossovers would likely not be representative of the large-scale behavior of the ice shelf due to the spatial variability of ice thickness change. Satellite altimetry measurements from ICESat-2 (Markus et al., 2017) should help rectify the data limitation problem by providing dense ~~point clouds which~~ and repeated point clouds. ICESat-2 data could be combined with photogrammetric digital elevation models (DEMs) to create high-resolution ice shelf-wide thickness change maps (Berger et al., 2017; Shean et al., 2018). ~~A more comprehensive update from the ICESat results of Pritchard et al. (2012) and Rignot et al. (2013) will be possible once ICESat-2 data become available.~~ Combining ICESat-2 with DEMs would help improve the use of the laser altimetry data in a Lagrangian reference frame as ice parcels could be accurately tracked between separate satellite tracks.

Here, the airborne data are co-registered in a Lagrangian reference frame using a static velocity map provided by NSIDC through the MEaSUREs program (Rignot et al., 2017). However, there are cases that do not fit the assumption of temporally-invariant velocities. Prior to the calving event of the 40,000 km^2 A-68 iceberg from the Larsen-C ~~ice shelf~~ Ice Shelf on July 11, 2017, the ice was rifting from the south and the regions downstream of the crack were rotating outward ~~(Hogg and Gudmundsson, 2017, Figure 5)~~(Hogg and Gudmundsson, 2017, Figure 6). In the Amundsen Sea Embayment, the ice velocity structure has changed year-to-year since the 1990's (Rignot et al., 2008; Mouginot et al., 2014). The floating ice shelves in the Amundsen Sea are also rifting concurrently with the acceleration of the instreaming glaciers (Macgregor et al., 2012). For both of these cases, it would be more appropriate to predict the advected parcel location using a velocity time seriestime-variable velocity maps. However, the spatial coverage of annual velocity maps is lacking for some time periods, which will complicate the advection calculation. With the high-temporal resolution data from the ESA Sentinel mission, the Landsat-based goLIVE project and the future NASA-ISRO SAR mission (NISAR), the advected parcel locations could be predicted with much greater accuracy for recent Operation IceBridge campaigns and future altimetry missions . (Fahnestock et al., 2016; Gardner et al., 2018; Mouginot et al., 2017a). Improvements in ice thickness and ice velocity estimates will also greatly improve estimates of flux divergence and as a consequence estimates of basal melt rates calculated using mass conservation (Berger et al., 2017; Adusumilli et al., 2018).

This work builds off of the work of Paolo et al. (2015) and Adusumilli et al. (2018) that used radar altimetry data to analyze the recent thinning and basal melt rates of ice shelves. Paolo et al. (2015) calculated changes in the ice thickness time series over an 18-year time period using a suite of satellite radar altimetry data compiled in an Eulerian frame of reference. They found that the overall volume loss of ice shelves accelerated over the period 1994–2012, particularly for the ice shelves of West Antarctica. Adusumilli et al. (2018) expanded on this work to estimate the basal melt rates over 23 years and including radar altimetry data from CryoSat-2. Our study provides a validation dataset for floating ice shelves using high-resolution airborne laser altimetry data. Laser altimeters and radar altimeters can measure different surfaces over snow-covered ice surfaces (Rémy and Parouty, 2009). Idealistically, the laser altimeter will detect the snow surface and the radar altimeter will detect the snow-ice interface. Because laser altimeters ideally detect the snow surface, an estimate of the total column snow/firn height change is needed to calculate the ice shelf freeboard change (Pritchard et al., 2012). For radar altimeters, the radar penetration depth is affected by variations Variations in the dielectric properties of the snow due to variable temperatures and snow grain sizes can affect the radar penetration depth(Rémy and Parouty, 2009). surface layer due to variations in temperature, snow grain size, snow density and moisture content (Partington et al., 1989; Rémy and Parouty, 2009). Due to the variations in penetration depth, estimates of the firn height change below the detected surface are necessary in order to calculate the freeboard change. Determining the sensitivity of radar estimates to surface penetration over different surface types could help reconcile differences between the various estimates. Our study provides a validation dataset for floating ice shelves using high-resolution airborne laser altimetry data (Figure 7).

Compiling estimates of elevation change from laser altimetry is non-trivial and different processing methods can produce differing results. Felikson et al. (2017) compared four different processing schemes (crossover differencing, along-track surface fits, overlapping footprints and triangulated irregular networks) using ICESat data in an Eulerian sense over grounded ice in Greenland. They found discernible and irreconcilable differences between methods when deriving elevation change over the grounded ice sheet. We compare results from overlapping footprints and triangulated irregular networks , the two methods most applicable to airborne data, to test their coherence over ice shelf surfaces. As the surface slopes on ice shelves are small, we find that overlapping footprints and TINs approaches produce similar estimates of elevation change with scanning lidars in Lagrangian frames of reference (Figure 4). The overlapping footprints approach produces a slightly noisier but statistically similar estimate compared with the TINs approach, and is a significantly simpler algorithm to implement.

5 Conclusions

We present a method for measuring ice shelf thickness change through the co-registration of Operation IceBridge laser altimetry data in a Lagrangian reference frame. We use our method to detect changes in ice shelves in West Antarctica and the Antarctic Peninsula where the airborne data are available. We find that our method is a significant improvement over Eulerian-derived estimates that require substantial smoothing or spatial averaging of the data. However, there are significant limitations when using airborne data for detecting ice shelf thickness change with Lagrangian tracking, particularly the lower spatial coverage and typical lack of repeat tracks over ice shelves. Data from the recently launched NASA ICESat-2 mission will help rectify these problems, particularly if combined with high-resolution photogrammetric digital elevation models.

Code and data availability. NASA Operation IceBridge data are freely available from the National Snow and Ice Data Center (NSIDC) at http://nsidc.org/data/ILATM2/ for the Level-2 ATM data and http://nsidc.org/data/ILVIS2/ for the Level-2 LVIS data. NASA MEaSUREs INSAR-derived velocity maps are provided by NSIDC at https://nsidc.org/data/nsidc-0484. Bedmap2 ice thicknesses are provided by the British Antarctic Survey at https://www.bas.ac.uk/project/bedmap-2/. CATS2008 tidal constituents are available from the Earth & Space Research institute at https://www.esr.org/research/polar-tide-models/. Dynamic atmospheric Corrections are produced by CLS Space Oceanography Division using the Mog2D model from Legos distributed by Aviso, with support from CNES. Ssalto/Duacs non-tidal sea surface products were produced and distributed by the Copernicus Marine and Environment Monitoring Service (CMEMS). Landsat imagery is provided courtesy of the U.S. Geological Survey EarthExplorer service. MODIS images of ice shelves are freely available from NSIDC. The following programs are provided by this project for processing the Operation IceBridge data: *nsidc-earthdata* retrieves NASA data from NSIDC, *read-ATM1b-QFIT-binary* reads Level-1b Airborne Topographic Mapper (ATM) QFIT binary data products, *read-ATM2-icessn* reads Level-2 ATM Icessn data products and *read-LVIS2-elevation* reads Level-2 Land Vegetation and Ice Sensor (LVIS) data products.

Author contributions. T.C.S. performed the analysis and wrote the manuscript. T.M. and T.A.N. supervised the project and provided comments and feedback. M.v.d.B, S.R.M.L. and J.M.v.W. supplied the RACMO2.3p2 data and provided comments.

Competing interests. The authors declare that the research was conducted in the absence of any commercial or financial relationships that could be construed as a potential conflict of interest.

Acknowledgements. Research was supported by an appointment to the NASA Postdoctoral Program at NASA Goddard Space Flight Center, administered by Universities Space Research Association under contract with NASA. The authors wish to thank the editor ~~and~~ Kenichi Matsuoka and the two anonymous reviewers for their comments ~~, Eric Rignot~~ and suggestions. We wish to thank Eric Rignot (UCI/JPL) and Isabella Velicogna (UCI/JPL) for their comments, Jeremie Mouginot (UCI) for his advice on the laser altimetry analysis, and members of the GSFC Cryospheric Sciences Laboratory for their comments and advice. The authors thank Susheel Adusumilli (UCSD/SIO) for providing the estimated basal melt rates of the Larsen-C ice shelf from radar altimetry data. The authors wish to acknowledge the NASA Operation IceBridge flight, instrument and science teams for their work to collect and produce the science data.

References

Adusumilli, S., Fricker, H. A., Siegfried, M. R., Padman, L., Paolo, F. S., and Ligtenberg, S. R. M.: Variable Basal Melt Rates of Antarctic Peninsula Ice Shelves, 1994–2016, Geophysical Research Letters, 45, 4086–4095, https://doi.org/10.1002/2017GL076652, https://doi.org/10.1002/2017GL076652, 2018.

Altamimi, Z., Rebischung, P., Métivier, L., and Collilieux, X.: ITRF2014: A new release of the International Terrestrial Reference Frame modeling nonlinear station motions, Journal of Geophysical Research: Solid Earth, 121, 6109–6131, https://doi.org/10.1002/2016JB013098, http://dx.doi.org/10.1002/2016JB013098, 2016JB013098, 2016.

Armitage, T. W. K., Kwok, R., Thompson, A. F., and Cunningham, G.: Dynamic Topography and Sea Level Anomalies of the Southern Ocean: Variability and Teleconnections, Journal of Geophysical Research: Oceans, 123, 613–630, https://doi.org/10.1002/2017JC013534, https://doi.org/10.1002/2017JC013534, 2018.

Berger, S., Drews, R., Helm, V., Sun, S., and Pattyn, F.: Detecting high spatial variability of ice shelf basal mass balance, Roi Baudouin Ice Shelf, Antarctica, The Cryosphere, 11, 2675–2690, https://doi.org/10.5194/tc-11-2675-2017, https://www.the-cryosphere.net/11/2675/2017/, 2017.

Berthier, E., Scambos, T. A., and Shuman, C. A.: Mass loss of Larsen B tributary glaciers (Antarctic Peninsula) unabated since 2002, Geophysical Research Letters, 39, https://doi.org/10.1029/2012GL051755, http://doi.wiley.com/10.1029/2012GL051755, l13501, 2012.

Blair, J. B. and Hofton, M.: IceBridge LVIS L2 Geolocated Surface Elevation Product, NASA DAAC at the National Snow and Ice Data Center, Boulder, Colorado USA, http://dx.doi.org/10.5067/OIKFGJNBM6OO, version 2, 2010.

Blair, J. B., Rabine, D. L., and Hofton, M. A.: The Laser Vegetation Imaging Sensor: a medium-altitude, digitisation-only, airborne laser altimeter for mapping vegetation and topography, ISPRS Journal of Photogrammetry and Remote Sensing, 54, 115–122, https://doi.org/10.1016/S0924-2716(99)00002-7, http://www.sciencedirect.com/science/article/pii/S0924271699000027, 1999.

Brunt, K. M., Fricker, H. A., Padman, L., Scambos, T. A., and O'Neel, S.: Mapping the grounding zone of the Ross Ice Shelf, Antarctica, using ICESat laser altimetry, Annals of Glaciology, 51, 71–79, https://doi.org/10.3189/172756410791392790, https://doi.org/10.3189/172756410791392790, 2010.

Brunt, K. M., Fricker, H. A., and Padman, L.: Analysis of ice plains of the Filchner–Ronne Ice Shelf, Antarctica, using ICESat laser altimetry, Journal of Glaciology, 57, 965–975, https://doi.org/10.3189/002214311798043753, http://dx.doi.org/10.3189/002214311798043753, 2011.

Carrère, L. and Lyard, F.: Modeling the barotropic response of the global ocean to atmospheric wind and pressure forcing - comparisons with observations, Geophysical Research Letters, 30, https://doi.org/10.1029/2002GL016473, http://dx.doi.org/10.1029/2002GL016473, 1275, 2003.

Church, J. A., White, N. J., Konikow, L. F., Domingues, C. M., Cogley, J. G., Rignot, E. J., Gregory, J. M., van den Broeke, M. R., Monaghan, A. J., and Velicogna, I.: Revisiting the Earth's sea-level and energy budgets from 1961 to 2008, Geophysical Research Letters, 38, https://doi.org/10.1029/2011GL048794, http://dx.doi.org/10.1029/2011GL048794, l18601, 2011.

CMEMS: Ssalto/Duacs altimeter products were produced and distributed by the Copernicus Marine and Environment Monitoring Service (CMEMS), http://www.marine.copernicus.eu, 2017.

Cuffey, K. M. and Paterson, W. S. B.: The Physics of Glaciers, Butterworth-Heinemann, Burlington, MA, 4th edn., http://www.elsevierdirect.com/ISBN/9780123694614/The-Physics-of-Glaciers, 2010.

Das, I., Bell, R. E., Scambos, T. A., Wolovick, M., Creyts, T. T., Studinger, M., Frearson, N., Nicolas, J. P., Lenaerts, J. T. M., and van den Broeke, M. R.: Influence of persistent wind scour on the surface mass balance of Antarctica, Nature Geoscience, 6, 367–371, https://doi.org/10.1038/ngeo1766, http://www.nature.com/doifinder/10.1038/ngeo1766, 2013.

Datta, R. T., Tedesco, M., Agosta, C., Fettweis, X., Kuipers Munneke, P., and van den Broeke, M. R.: Melting over the northeast Antarctic Peninsula (1999–2009): evaluation of a, The Cryosphere, 12, 2901–2922, https://doi.org/10.5194/tc-12-2901-2018, https://www.the-cryosphere.net/12/2901/2018/, 2018.

Depoorter, M. A., Bamber, J. L., Griggs, J. A., Lenaerts, J. T. M., Ligtenberg, S. R. M., van den Broeke, M. R., and Moholdt, G.: Calving fluxes and basal melt rates of Antarctic ice shelves, Nature, 502, 89–92, https://doi.org/10.1038/nature12567, http://dx.doi.org/10.1038/nature12567, 2013.

Desai, S. D.: Observing the pole tide with satellite altimetry, Journal of Geophysical Research: Oceans, 107, 7–1–7–13, https://doi.org/10.1029/2001JC001224, http://dx.doi.org/10.1029/2001JC001224, 3186, 2002.

Dupont, T. and Alley, R. B.: Assessment of the importance of ice-shelf buttressing to ice-sheet flow, Geophysical Research Letters, 32, https://doi.org/10.1029/2004GL022024, http://dx.doi.org/10.1029/2004GL022024, l04503, 2005.

Dutrieux, P., De Rydt, J., Jenkins, A., Holland, P. R., Ha, H. K., Lee, S. H., Steig, E. J., Ding, Q., Abrahamsen, E., and Schröder, M.: Strong Sensitivity of Pine Island Ice-Shelf Melting to Climatic Variability, Science, 343, 174–178, https://doi.org/10.1126/science.1244341, http://science.sciencemag.org/content/343/6167/174, 2014.

Fahnestock, M., Scambos, T., Moon, T., Gardner, A., Haran, T., and Klinger, M.: Rapid large-area mapping of ice flow using Landsat 8, Remote Sensing of Environment, 185, 84–94, https://doi.org/10.1016/j.rse.2015.11.023, http://dx.doi.org/10.1016/j.rse.2015.11.023, 2016.

Felikson, D., Urban, T. J., Gunter, B. C., Pie, N., Pritchard, H. D., Harpold, R., and Schutz, B. E.: Comparison of Elevation Change Detection Methods From ICESat Altimetry Over the Greenland Ice Sheet, IEEE Transactions on Geoscience and Remote Sensing, PP, 1–12, https://doi.org/10.1109/TGRS.2017.2709303, 2017.

Flament, T. and Rémy, F.: Dynamic thinning of Antarctic glaciers from along-track repeat radar altimetry, Journal of Glaciology, 58, 830–840, https://doi.org/10.3189/2012JoG11J118, http://dx.doi.org/10.3189/2012JoG11J118, 2012.

Fretwell, P., Pritchard, H. D., Vaughan, D. G., Bamber, J. L., Barrand, N. E., Bell, R. E., Bianchi, C., Bingham, R. G., Blankenship, D. D., Casassa, G., Catania, G. A., Callens, D., Conway, H., Cook, A. J., Corr, H. F. J., Damaske, D., Damm, V., Ferraccioli, F., Forsberg, R., Fujita, S., Gim, Y., Gogineni, S. P., Griggs, J. A., Hindmarsh, R. C. A., Holmlund, P., Holt, J. W., Jacobel, R. W., Jenkins, A., Jokat, W., Jordan, T. A., King, E. C., Kohler, J., Krabill, W. B., Riger-Kusk, M., Langley, K. A., Leitchenkov, G., Leuschen, C., Luyendyk, B. P., Matsuoka, K., Mouginot, J., Nitsche, F. O., Nogi, Y., Nost, O. A., Popov, S. V., Rignot, E. J., Rippin, D. M., Rivera, A., Roberts, J. L., Ross, N., Siegert, M. J., Smith, A. M., Steinhage, D., Studinger, M., Sun, B., Tinto, B. K., Welch, B. C., Wilson, D., Young, D. A., Xiangbin, C., and Zirizzotti, A.: Bedmap2: improved ice bed, surface and thickness datasets for Antarctica, The Cryosphere, 7, 375–393, https://doi.org/10.5194/tc-7-375-2013, http://www.the-cryosphere.net/7/375/2013/, 2013.

Fricker, H. A. and Padman, L.: Thirty years of elevation change on Antarctic Peninsula ice shelves from multimission satellite radar altimetry, Journal of Geophysical Research: Oceans, 117, https://doi.org/10.1029/2011JC007126, http://dx.doi.org/10.1029/2011JC007126, c02026, 2012.

Fricker, H. A., Popov, S., Allison, I., and Young, N.: Distribution of marine ice beneath the Amery Ice Shelf, Geophysical Research Letters, 28, 2241–2244, https://doi.org/10.1029/2000GL012461, http://dx.doi.org/10.1029/2000GL012461, 2001.

Gardner, A. S., Moholdt, G., Scambos, T., Fahnstock, M., Ligtenberg, S., van den Broeke, M., and Nilsson, J.: Increased West Antarctic and unchanged East Antarctic ice discharge over the last 7 years, The Cryosphere, 12, 521–547, https://doi.org/10.5194/tc-12-521-2018, https://www.the-cryosphere.net/12/521/2018/, 2018.

Griggs, J. A. and Bamber, J. L.: Antarctic ice-shelf thickness from satellite radar altimetry, Journal of Glaciology, 57, 485–498, https://doi.org/10.3189/002214311796905659, http://dx.doi.org/10.3189/002214311796905659, 2011.

Haran, T., Bohlander, J., Scambos, T., and Fahnestock, M.: MODIS Mosaic of Antarctica 2008-2009 (MOA2009) Image Map, NSIDC: National Snow and Ice Data Center, Boulder, Colorado USA, https://doi.org/10.7265/N5KP8037, http://dx.doi.org/10.7265/N5KP8037, version 1, 2014.

Hofton, M. A., Blair, J. B., Luthcke, S. B., and Rabine, D. L.: Assessing the performance of 20–25 m footprint waveform lidar data collected in ICESat data corridors in Greenland, Geophysical Research Letters, 35, https://doi.org/10.1029/2008GL035774, http://dx.doi.org/10.1029/2008GL035774, l24501, 2008.

Hogg, A. E. and Gudmundsson, G. H.: Impacts of the Larsen-C Ice Shelf calving event, Nature Climate Change, 7, 540, https://doi.org/10.1038/nclimate3359, http://dx.doi.org/10.1038/nclimate3359, 2017.

Jacobs, S. S., Jenkins, A., Giulivi, C. F., and Dutrieux, P.: Stronger ocean circulation and increased melting under Pine Island Glacier ice shelf, Nature Geoscience, 4, 519–523, https://doi.org/10.1038/ngeo1188, http://dx.doi.org/10.1038/ngeo1188, 2011.

Jenkins, A., Shoosmith, D., Dutrieux, P., Jacobs, S., Kim, T. W., Lee, S. H., Ha, H. K., and Stammerjohn, S.: West Antarctic Ice Sheet retreat in the Amundsen Sea driven by decadal oceanic variability, Nature Geoscience, 11, 733–738, https://doi.org/10.1038/s41561-018-0207-4, https://doi.org/10.1038/s41561-018-0207-4, 2018.

Khazendar, A., Rignot, E. J., Schroeder, D. M., Seroussi, H., Schodlok, M. P., Scheuchl, B., Mouginot, J., Sutterley, T. C., and Velicogna, I.: Rapid submarine ice melting in the grounding zones of ice shelves in West Antarctica, Nature Communications, 7, 13 243, https://doi.org/10.1038/ncomms13243, http://dx.doi.org/10.1038/ncomms13243, 2016.

King, M. A., Padman, L., Nicholls, K., Clarke, P. J., Gudmundsson, G., Kulessa, B., and Shepherd, A.: Ocean tides in the Weddell Sea: New observations on the Filchner-Ronne and Larsen C ice shelves and model validation, Journal of Geophysical Research: Oceans, 116, https://doi.org/10.1029/2011JC006949, http://dx.doi.org/10.1029/2011JC006949, c06006, 2011.

Kuipers Munneke, P., McGrath, D., Medley, B., Luckman, A., Bevan, S., Kulessa, B., Jansen, D., Booth, A., Smeets, P., Hubbard, B., Ashmore, D., Van den Broeke, M., Sevestre, H., Steffen, K., Shepherd, A., and Gourmelen, N.: Observationally constrained surface mass balance of Larsen C ice shelf, Antarctica, The Cryosphere, 11, 2411–2426, https://doi.org/10.5194/tc-11-2411-2017, https://www.the-cryosphere.net/11/2411/2017/, 2017.

Le Traon, P. Y., Nadal, F., and Ducet, N.: An Improved Mapping Method of Multisatellite Altimeter Data, Journal of Atmospheric and Oceanic Technology, 15, 522–534, https://doi.org/10.1175/1520-0426(1998)015<0522:AIMMOM>2.0.CO;2, http://dx.doi.org/10.1175/1520-0426(1998)015<0522:aimmom>2.0.co;2, 1998.

Legos: Dynamic atmospheric Corrections are produced by CLS Space Oceanography Division using the Mog2D model from Legos distributed by Aviso, with support from CNES, https://www.aviso.altimetry.fr/en/data/products/auxiliary-products/atmospheric-corrections.html, 2017.

Lenaerts, J. T. M., van den Broeke, M. R., van de Berg, W. J., van Meijgaard, E., and Kuipers Munneke, P.: A new, high-resolution surface mass balance map of Antarctica (1979–2010) based on regional atmospheric climate modeling, Geophysical Research Letters, 39, https://doi.org/10.1029/2011GL050713, http://dx.doi.org/10.1029/2011GL050713, l04501, 2012.

Lenaerts, J. T. M., Ligtenberg, S. R. M., Medley, B., Van de Berg, W. J., Konrad, H., Nicolas, J. P., Van Wessem, J. M., Trusel, L. D., Mulvaney, R., Tuckwell, R. J., Hogg, A. E., and Thomas, E. R.: Climate and surface mass balance of coastal West Antarctica resolved by regional climate modelling, Annals of Glaciology, 59, 29–41, https://doi.org/10.1017/aog.2017.42, https://doi.org/10.1017/aog.2017.42, 2018.

Ligtenberg, S. R. M., Helsen, M. M., and van den Broeke, M. R.: An improved semi-empirical model for the densification of Antarctic firn, The Cryosphere, 5, 809–819, https://doi.org/10.5194/tc-5-809-2011, http://www.the-cryosphere.net/5/809/2011/, 2011.

Ligtenberg, S. R. M., Horwath, M., van den Broeke, M. R., and Legrésy, B.: Quantifying the seasonal "breathing" of the Antarctic ice sheet, Geophysical Research Letters, 39, https://doi.org/10.1029/2012GL053628, http://dx.doi.org/10.1029/2012GL053628, l23501, 2012.

Ligtenberg, S. R. M., Berg, W. J., van den Broeke, M. R., Rae, J. G. L., and van Meijgaard, E.: Future surface mass balance of the Antarctic ice sheet and its influence on sea level change, simulated by a regional atmospheric climate model, Climate Dynamics, 41, 867–884, https://doi.org/10.1007/s00382-013-1749-1, http://dx.doi.org/10.1007/s00382-013-1749-1, 2013.

Lilien, D. A., Joughin, I., Smith, B., and Shean, D. E.: Changes in flow of Crosson and Dotson ice shelves, West Antarctica, in, The Cryosphere, 12, 1415–1431, https://doi.org/10.5194/tc-12-1415-2018, https://www.the-cryosphere.net/12/1415/2018/, 2018.

LPDAAC: NASA Landsat Program, NASA EOSDIS Land Processes Distributed Active Archive Center (LP DAAC), USGS/Earth Resources Observation and Science (EROS) Center, Sioux Falls, South Dakota, https://lpdaac.usgs.gov/, 2017.

Lynch, D. R. and Gray, W. G.: A wave equation model for finite element tidal computations, Computers & Fluids, 7, 207–228, https://doi.org/10.1016/0045-7930(79)90037-9, http://www.sciencedirect.com/science/article/pii/0045793079900379, 1979.

Macgregor, J. A., Catania, G. A., Markowski, M. S., and Andrews, A. G.: Widespread rifting and retreat of ice-shelf margins in the eastern Amundsen Sea Embayment between 1972 and 2011, Journal of Glaciology, 58, 458–466, https://doi.org/10.3189/2012JoG11J262, http://dx.doi.org/10.3189/2012jog11j262, 2012.

Markus, T., Neumann, T., Martino, A., Abdalati, W., Brunt, K., Csatho, B., Farrell, S., Fricker, H., Gardner, A., Harding, D., Jasinski, M., Kwok, R., Magruder, L., Lubin, D., Luthcke, S., Morison, J., Nelson, R., Neuenschwander, A., Palm, S., Popescu, S., Shum, C., Schutz, B. E., Smith, B., Yang, Y., and Zwally, J.: The Ice, Cloud, and land Elevation Satellite-2 (ICESat-2): Science requirements, concept, and implementation, Remote Sensing of Environment, 190, 260–273, https://doi.org/10.1016/j.rse.2016.12.029, https://doi.org/10.1016/j.rse.2016.12.029, 2017.

McMillan, M., Shepherd, A., Sundal, A. V., Briggs, K. H., Muir, A., Ridout, A., Hogg, A., and Wingham, D.: Increased ice losses from Antarctica detected by CryoSat-2, Geophysical Research Letters, 41, 3899–3905, https://doi.org/10.1002/2014GL060111, http://dx.doi.org/10.1002/2014GL060111, 2014GL060111, 2014.

Medley, B., Joughin, I. R., Smith, B. E., Das, S. B., Steig, E. J., Conway, H., Gogineni, S. P., Lewis, C., Criscitiello, A. S., McConnell, J. R., van den Broeke, M. R., Lenaerts, J. T. M., Bromwich, D. H., Nicolas, J. P., and Leuschen, C.: Constraining the recent mass balance of Pine Island and Thwaites glaciers, West Antarctica, with airborne observations of snow accumulation, The Cryosphere, 8, 1375–1392, https://doi.org/10.5194/tc-8-1375-2014, http://www.the-cryosphere.net/8/1375/2014/, 2014.

Moholdt, G., Padman, L., and Fricker, H. A.: Basal mass budget of Ross and Filchner-Ronne ice shelves, Antarctica, derived from Lagrangian analysis of ICESat altimetry, Journal of Geophysical Research: Earth Surface, 119, 2361–2380, https://doi.org/10.1002/2014JF003171, http://dx.doi.org/10.1002/2014JF003171, 2014JF003171, 2014.

Mouginot, J., Rignot, E. J., and Scheuchl, B.: Sustained increase in ice discharge from the Amundsen Sea Embayment, West Antarctica, from 1973 to 2013, Geophysical Research Letters, 41, 1576–1584, https://doi.org/10.1002/2013GL059069, http://dx.doi.org/10.1002/2013GL059069, 2014.

Mouginot, J., Rignot, E., Scheuchl, B., and Millan, R.: Comprehensive Annual Ice Sheet Velocity Mapping Using Landsat-8, Sentinel-1, and RADARSAT-2 Data, Remote Sensing, 9, https://doi.org/10.3390/rs9040364, http://www.mdpi.com/2072-4292/9/4/364, 364, 2017a.

Mouginot, J., Scheuchl, B., and Rignot, E.: MEaSUREs Antarctic Boundaries for IPY 2007–2009 from Satellite Radar, NASA National Snow and Ice Data Center Distributed Active Archive Center, Boulder, Colorado USA, https://doi.org/10.5067/AXE4121732AD, http://dx.doi.org/10.5067/AXE4121732AD, version 2, 2017b.

Neumann, T., Brenner, A., Hancock, D., Robbins, J., and Saba, J.: Ice, Cloud, and land Elevation Satellite - 2 (ICESat-2) Project: Algorithm Theoretical Basis Document (ATBD) for Global Geolocated Photons (ATL03), Tech. rep., NASA Goddard Space Flight Center (GSFC), Greenbelt, MD, USA, https://icesatiimis.gsfc.nasa.gov, 2018.

Padman, L., Fricker, H. A., Coleman, R., Howard, S., and Erofeeva, L.: A new tide model for the Antarctic ice shelves and seas, Annals of Glaciology, 34, 247–254, https://doi.org/10.3189/172756402781817752, http://dx.doi.org/10.3189/172756402781817752, 2002.

Padman, L., Erofeeva, S. Y., and Fricker, H. A.: Improving Antarctic tide models by assimilation of ICESat laser altimetry over ice shelves, Geophysical Research Letters, 35, https://doi.org/10.1029/2008GL035592, http://dx.doi.org/10.1029/2008GL035592, l22504, 2008.

Padman, L., Costa, D. P., Dinniman, M. S., Fricker, H. A., Goebel, M. E., Huckstadt, L. A., Humbert, A., Joughin, I. R., Lenaerts, J. T. M., Ligtenberg, S. R. M., Scambos, T. A., and van den Broeke, M. R.: Oceanic controls on the mass balance of Wilkins Ice Shelf, Antarctica, Journal of Geophysical Research: Oceans, 117, https://doi.org/10.1029/2011JC007301, http://dx.doi.org/10.1029/2011JC007301, c01010, 2012.

Paolo, F. S., Fricker, H. A., and Padman, L.: Volume loss from Antarctic ice shelves is accelerating, Science, 348, 327–331, https://doi.org/10.1126/science.aaa0940, http://science.sciencemag.org/content/348/6232/327.abstract, 2015.

Paolo, F. S., Fricker, H. A., and Padman, L.: Constructing improved decadal records of Antarctic ice shelf height change from multiple satellite radar altimeters, Remote Sensing of Environment, 177, 192–205, https://doi.org/10.1016/j.rse.2016.01.026, http://linkinghub.elsevier.com/retrieve/pii/S0034425716300268, 2016.

Partington, K. C., Ridley, J. K., Rapley, C. G., and Zwally, H. J.: Observations of the Surface Properties of the Ice Sheets by Satellite Radar Altimetry, Journal of Glaciology, 35, 267–275, https://doi.org/10.3189/S0022143000004603, https://doi.org/10.3189/S0022143000004603, 1989.

Petit, G. and Luzum, B.: IERS Conventions (2010), Tech. Rep. 36, International Earth Rotation and Reference Systems Service (IERS), Frankfurt am Main: Verlag des Bundesamts für Kartographie und Geodäsie, https://www.iers.org/IERS/EN/Publications/TechnicalNotes/tn36.html, 2010.

Pritchard, H. D., Arthern, R. J., Vaughan, D. G., and Edwards, L. A.: Extensive dynamic thinning on the margins of the Greenland and Antarctic ice sheets, Nature, 461, 971–975, https://doi.org/10.1038/nature08471, http://www.nature.com/nature/journal/vaop/ncurrent/full/nature08471.html), 2009.

Pritchard, H. D., Ligtenberg, S. R. M., Fricker, H. A., Vaughan, D. G., van den Broeke, M. R., and Padman, L.: Antarctic ice-sheet loss driven by basal melting of ice shelves, Nature, 484, 502–505, https://doi.org/10.1038/nature10968, http://www.nature.com/doifinder/10.1038/nature10968, 2012.

Ray, R. D.: A global ocean tide model from Topex/Poseidon altimetry: GOT99.2, Tech. Rep. TM-1999-209478, NASA Goddard Space Flight Center, Greenbelt, MD, http://ntrs.nasa.gov/archive/nasa/casi.ntrs.nasa.gov/19990089548_1999150788.pdf, 1999.

Rémy, F. and Parouty, S.: Antarctic Ice Sheet and Radar Altimetry: A Review, Remote Sensing, 1, 1212–1239, https://doi.org/10.3390/rs1041212, http://www.mdpi.com/2072-4292/1/4/1212/, 2009.

Ries, J., Bettadpur, S., Eanes, R., Kang, Z., Ko, U., McCullough, C., Nagel, P., Pie, N., Poole, S., Richter, T., Save, H., and Tapley, B.: The Development and Evaluation of the Global Gravity Model GGM05, Tech. Rep. CSR-16-02, UTCSR, Austin, Texas, https://doi.org/10.5880/icgem.2016.002, ftp://ftp.csr.utexas.edu/pub/grace/GGM05/CSR-16-02.pdf, 2016.

Rignot, E.: Ice-shelf changes in Pine Island Bay, Antarctica, 1947–2000, Journal of Glaciology, 48, 247–256, https://doi.org/10.3189/172756502781831386, http://dx.doi.org/10.3189/172756502781831386, 2002.

Rignot, E. J. and Jacobs, S.: Rapid Bottom Melting Widespread near Antarctic Ice Sheet Grounding Lines, Science, 296, 2020–2023, https://doi.org/10.1126/science.1070942, http://www.sciencemag.org/cgi/doi/10.1126/science.1070942, 2002.

Rignot, E. J., Vaughan, D. G., Schmeltz, M., Dupont, T., and MacAyeal, D. R.: Acceleration of Pine Island and Thwaites Glaciers, West Antarctica, Annals of Glaciology, 34, 189–194, https://doi.org/10.3189/172756402781817950, http://dx.doi.org/10.3189/172756402781817950, 2002.

Rignot, E. J., Casassa, G., Gogineni, S. P., Krabill, W. B., Rivera, A., and Thomas, R. H.: Accelerated ice discharge from the Antarctic Peninsula following the collapse of Larsen B ice shelf, Geophysical Research Letters, 31, https://doi.org/10.1029/2004GL020697, http://dx.doi.org/10.1029/2004GL020697, l18401, 2004.

Rignot, E. J., Bamber, J. L., van den Broeke, M. R., Davis, C. H., Li, Y., van de Berg, W. J., and van Meijgaard, E.: Recent Antarctic ice mass loss from radar interferometry and regional climate modelling, Nature Geoscience, 1, 106–110, https://doi.org/10.1038/ngeo102, http://www.nature.com/ngeo/journal/v1/n2/abs/ngeo102.html, 2008.

Rignot, E. J., Jacobs, S., Mouginot, J., and Scheuchl, B.: Ice-Shelf Melting Around Antarctica, Science, 341, 266–270, https://doi.org/10.1126/science.1235798, http://science.sciencemag.org/content/341/6143/266, 2013.

Rignot, E. J., Mouginot, J., Morlighem, M., Seroussi, H., and Scheuchl, B.: Widespread, rapid grounding line retreat of Pine Island, Thwaites, Smith, and Kohler glaciers, West Antarctica, from 1992 to 2011, Geophysical Research Letters, 41, 3502–3509, https://doi.org/10.1002/2014GL060140, http://dx.doi.org/10.1002/2014GL060140, 2014.

Rignot, E. J., Mouginot, J., and Scheuchl, B.: MEaSUREs Antarctic Grounding Line from Differential Satellite Radar Interferometry, NASA National Snow and Ice Data Center Distributed Active Archive Center, Boulder, Colorado USA, https://doi.org/10.5067/IKBWW4RYHF1Q, http://dx.doi.org/10.5067/IKBWW4RYHF1Q, version 2, 2016.

Rignot, E. J., Mouginot, J., and Scheuchl, B.: MEaSUREs InSAR-Based Antarctica Ice Velocity Map, NASA National Snow and Ice Data Center Distributed Active Archive Center, Boulder, Colorado USA, https://doi.org/10.5067/D7GK8F5J8M8R, http://dx.doi.org/10.5067/D7GK8F5J8M8R, version 2, 2017.

Rott, H., Rack, W., Skvarca, P., and De Angelis, H.: Northern Larsen Ice Shelf, Antarctica: further retreat after collapse, Annals of Glaciology, 34, 277–282, https://doi.org/10.3189/172756402781817716, https://doi.org/10.3189/172756402781817716, 2002.

Rott, H., Müller, F., Nagler, T., and Floricioiu, D.: The imbalance of glaciers after disintegration of Larsen-B ice shelf, Antarctic Peninsula, The Cryosphere, 5, 125–134, https://doi.org/10.5194/tc-5-125-2011, http://www.the-cryosphere.net/5/125/2011/, 2011.

Savitzky, A. and Golay, M. J. E.: Smoothing and Differentiation of Data by Simplified Least Squares Procedures., Analytical Chemistry, 36, 1627–1639, https://doi.org/10.1021/ac60214a047, http://dx.doi.org/10.1021/ac60214a047, 1964.

Scambos, T., Raup, B. H., and Bohlander, J.: Images of Antarctic Ice Shelves, NASA National Snow and Ice Data Center Distributed Active Archive Center, Boulder, Colorado USA, https://doi.org/10.7265/N5NC5Z4N, http://dx.doi.org/10.7265/N5NC5Z4N, version 1, 2001.

Scambos, T., Fricker, H. A., Liu, C.-C., Bohlander, J., Fastook, J., Sargent, A., Massom, R., and Wu, A.-M.: Ice shelf disintegration by plate bending and hydro-fracture: Satellite observations and model results of the 2008 Wilkins ice shelf break-ups, Earth and Planetary Science Letters, 280, 51–60, https://doi.org/10.1016/j.epsl.2008.12.027, http://dx.doi.org/10.1016/j.epsl.2008.12.027, 2009.

Scheuchl, B., Mouginot, J., Rignot, E. J., Morlighem, M., and Khazendar, A.: Grounding line retreat of Pope, Smith, and Kohler Glaciers, West Antarctica, measured with Sentinel-1a radar interferometry data, Geophysical Research Letters, 43, 8572–8579, https://doi.org/10.1002/2016GL069287, http://dx.doi.org/10.1002/2016GL069287, 2016GL069287, 2016.

Shean, D. E., Joughin, I. R., Dutrieux, P., Smith, B. E., and Berthier, E.: Ice shelf basal melt rates from a high-resolution DEM record for Pine Island Glacier, Antarctica, The Cryosphere Discussions, 2018, 1–39, https://doi.org/10.5194/tc-2018-209, https://www.the-cryosphere-discuss.net/tc-2018-209/, 2018.

Shepherd, A., Wingham, D. J., Payne, T., and Skvarca, P.: Larsen Ice Shelf Has Progressively Thinned, Science, 302, 856–859, https://doi.org/10.1126/science.1089768, http://science.sciencemag.org/content/302/5646/856, 2003.

Slobbe, D. C., Lindenbergh, R. C., and Ditmar, P.: Estimation of volume change rates of Greenland's ice sheet from ICESat data using overlapping footprints, Remote Sensing of Environment, 112, 4204–4213, https://doi.org/10.1016/j.rse.2008.07.004, http://www.sciencedirect.com/science/article/pii/S0034425708002277, 2008.

Smith, B. E., Gourmelen, N., Huth, A., and Joughin, I.: Connected subglacial lake drainage beneath Thwaites Glacier, West Antarctica, The Cryosphere, 11, 451–467, https://doi.org/10.5194/tc-11-451-2017, http://www.the-cryosphere.net/11/451/2017/, 2017.

Studinger, M. S.: IceBridge ATM L2 Icessn Elevation, Slope, and Roughness, NASA National Snow and Ice Data Center Distributed Active Archive Center, Boulder, Colorado USA, https://doi.org/10.5067/CPRXXK3F39RV, http://dx.doi.org/10.5067/CPRXXK3F39RV, version 2, 2014.

Sutterley, T. C., Velicogna, I., Fettweis, X., Rignot, E., Noël, B., and van den Broeke, M.: Evaluation of Reconstructions of Snow/Ice Melt in Greenland by Regional Atmospheric Climate Models Using Laser Altimetry Data, Geophysical Research Letters, 45, 8324–8333, https://doi.org/10.1029/2018GL078645, https://doi.org/10.1029/2018GL078645, 2018.

Thomas, R. H.: Ice Shelves: A Review, Journal of Glaciology, 24, 273–286, https://doi.org/10.1017/S0022143000014799, https://www.cambridge.org/core/article/ice-shelves-a-review/A59D20319A6E15DB7A5C162BE4A0BF83, 1979.

Thomas, R. H. and Studinger, M. S.: Pre-IceBridge ATM L2 Icessn Elevation, Slope, and Roughness, NASA National Snow and Ice Data Center Distributed Active Archive Center, Boulder, Colorado USA, https://doi.org/10.5067/6C6WA3R918HJ, http://dx.doi.org/10.5067/6C6WA3R918HJ, version 1, 2010.

van de Berg, W. J., van den Broeke, M. R., Reijmer, C. H., and van Meijgaard, E.: Reassessment of the Antarctic surface mass balance using calibrated output of a regional atmospheric climate model, Journal of Geophysical Research: Atmospheres, 111, https://doi.org/10.1029/2005JD006495, http://dx.doi.org/10.1029/2005JD006495, d11104, 2006.

van den Broeke, M. R., Bamber, J. L., Ettema, J., Rignot, E. J., Schrama, E., van de Berg, W. J., van Meijgaard, E., Velicogna, I., and Wouters, B.: Partitioning Recent Greenland Mass Loss, Science, 326, 984–986, https://doi.org/10.1126/science.1178176, http://www.sciencemag.org/cgi/doi/10.1126/science.1178176, 2009.

van Wessem, J. M., Reijmer, C. H., Morlighem, M., Mouginot, J., Rignot, E. J., Medley, B., Joughin, I. R., Wouters, B., Depoorter, M. A., Bamber, J. L., Lenaerts, J. T. M., van de Berg, W. J., van den Broeke, M. R., and van Meijgaard, E.: Improved representation of East Antarctic surface mass balance in a regional atmospheric climate model, Journal of Glaciology, 60, 761–770, https://doi.org/10.3189/2014JoG14J051, http://dx.doi.org/10.3189/2014JoG14J051, 2014.

van Wessem, J. M., Ligtenberg, S. R. M., Reijmer, C. H., van de Berg, W. J., van den Broeke, M. R., Barrand, N. E., Thomas, E. R., Turner, J., Wuite, J., Scambos, T. A., and van Meijgaard, E.: The modelled surface mass balance of the Antarctic Peninsula at 5.5 km horizontal resolution, The Cryosphere, 10, 271–285, https://doi.org/10.5194/tc-10-271-2016, http://www.the-cryosphere.net/10/271/2016/, 2016.

van Wessem, J. M., van de Berg, W. J., Noël, B. P. Y., van Meijgaard, E., Amory, C., Birnbaum, G., Jakobs, C. L., Krüger, K., Lenaerts, J. T. M., Lhermitte, S., Ligtenberg, S. R. M., Medley, B., Reijmer, C. H., van Tricht, K., Trusel, L. D., van Ulft, L. H., Wouters, B., Wuite, J., and van den Broeke, M. R.: Modelling the climate and surface mass balance of polar ice sheets using RACMO2 – Part 2: Antarctica (1979–2016), The Cryosphere, 12, 1479–1498, https://doi.org/10.5194/tc-12-1479-2018, https://www.the-cryosphere.net/12/1479/2018/, 2018.

Vaughan, D. G., Mantripp, D. R., Sievers, J., and Doake, C. S.: A synthesis of remote sensing data on Wilkins Ice Shelf, Antarctica, Annals of Glaciology, 17, 211–218, https://doi.org/10.3189/S0260305500012866, http://dx.doi.org/10.3189/s0260305500012866, 1993.

Zwally, H. J. and Li, J.: Seasonal and interannual variations of firn densification and ice-sheet surface elevation at the Greenland summit, Journal of Glaciology, 48, 199–207, https://doi.org/10.3189/172756502781831403, http://dx.doi.org/10.3189/172756502781831403, 2002.

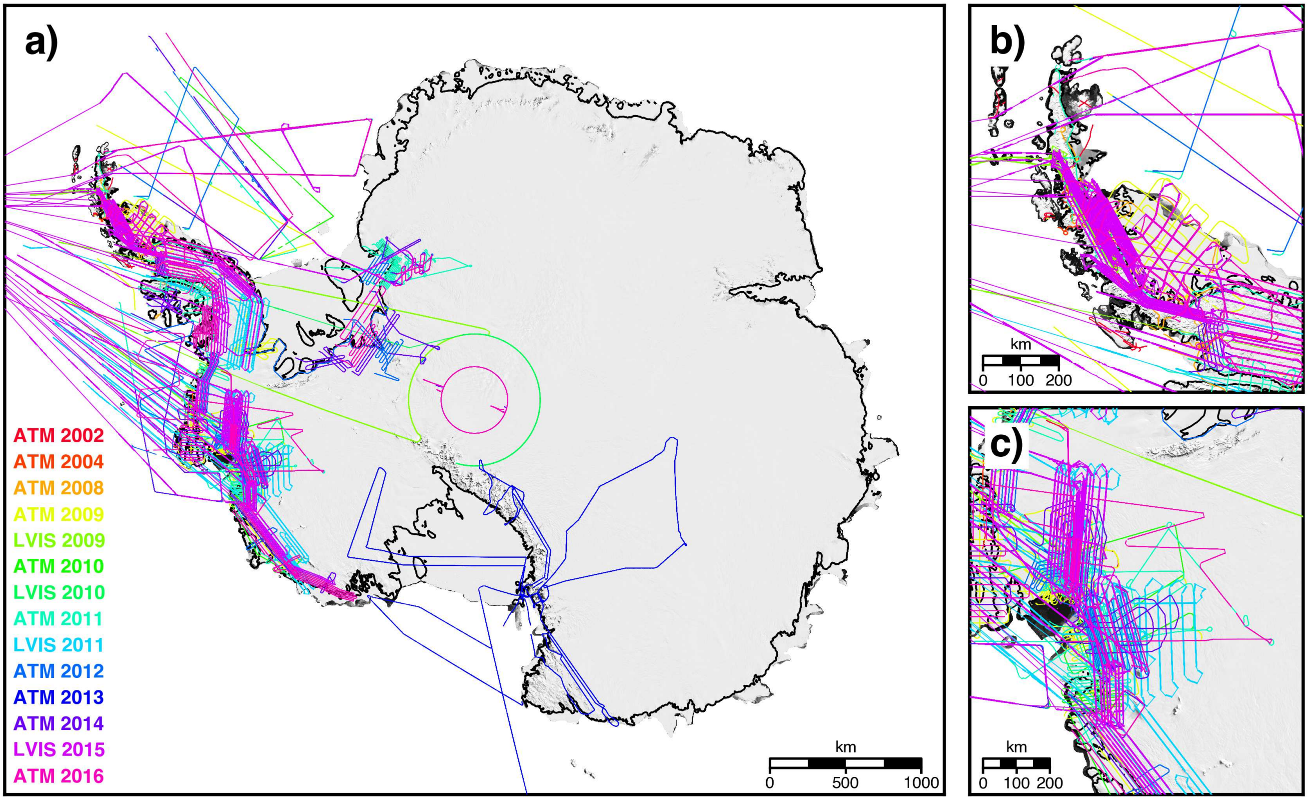

Figure 1. Pre-IceBridge and Operation IceBridge campaign flight lines over a) Antarctica b) the Antarctic Peninsula and c) the Amundsen Sea Embayment from 2002 to 2016 colored by year of acquisition and laser ranging instrument. Antarctic grounded ice delineation provided by Mouginot et al. (2017b). Flight lines overlaid on a 2008–2009 MODIS mosaic of Antarctica (Haran et al., 2014).

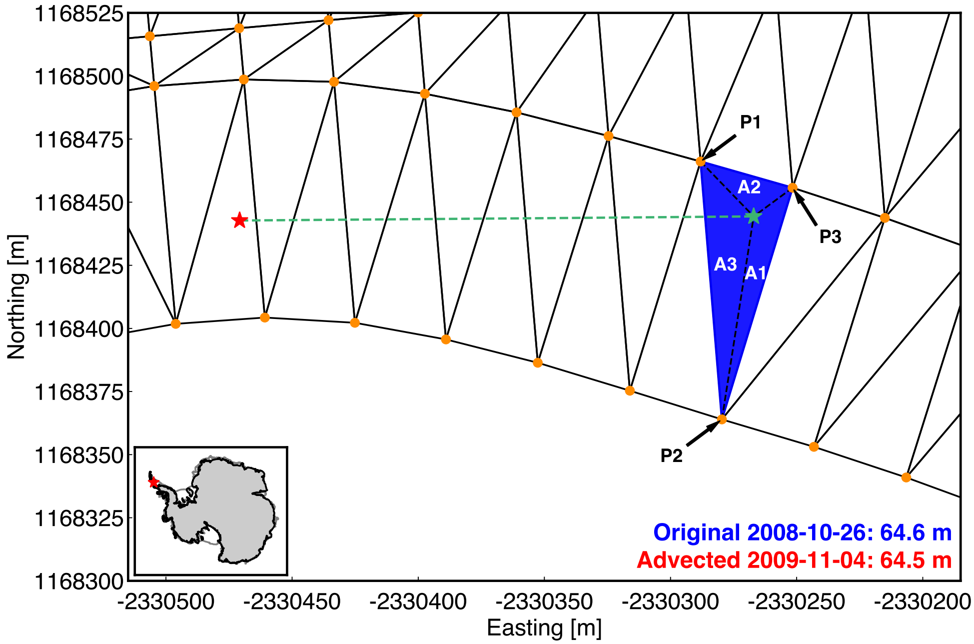

Figure 2. Triangulated mesh formulated around an advected 2008 ATM flight line point using points from a 2009 ATM flight line (orange dots). The red star denotes the location of the original point, the green star denotes the parcel location after advection, and the dashed green line is the path of advection. P1, P2 and P3 represent the three vertices of the triangle housing the advected ATM point. Elevation values at each vertex point are weighted in the interpolation by their respective areas, A1, A2 and A3. Inset map shows the location of the main figure.

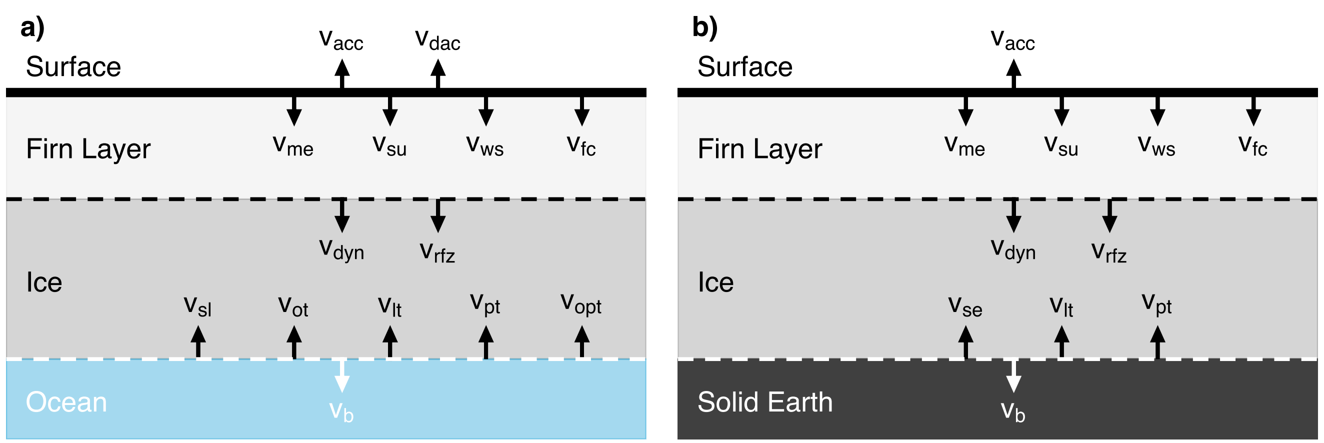

Figure 3. Representation of processes contributing to surface elevation changes for a) ice shelves and b) grounded ice. Modified from Ligtenberg et al. (2011) and Zwally and Li (2002). Processes represented in schematic: accumulation (v_{acc}), dynamic atmosphere (v_{dac}), snowmelt (v_{me}), sublimation (v_{su}), wind scour (v_{ws}), firn compaction (v_{fc}), ice dynamics (v_{dyn}), meltwater refreeze and retainment (v_{rfz}), solid Earth uplift (v_{se}), sea level (v_{sl}), ocean tides (v_{ot}), load tides (v_{lt}), load pole tides (v_{pt}), ocean pole tides (v_{opt}), and basal melt (v_b).

~~Ice thickness change (a-b) and estimated basal thickness change rates (c-d) of the Larsen-B remnant and Larsen-C ice shelf for two periods, 2002–2008 and 2008–2016. AI, CI, MI, WI and MOI denote the Adie, Cabinet, Mill, Whirlwind and Mobiloil inlets respectively. MEaSUREs InSAR-derived Antarctic grounded ice boundaries are denoted in gray (Mouginot et al., 2017b). 2016 and 2017 ice shelf extents delineated from MODIS imagery are denoted in green and light gray respectively (Scambos et al., 2001). Plots are overlaid on a 2008–2009 MODIS mosaic of Antarctica (Haran et al., 2014). Inset map denotes the location of the maps.~~

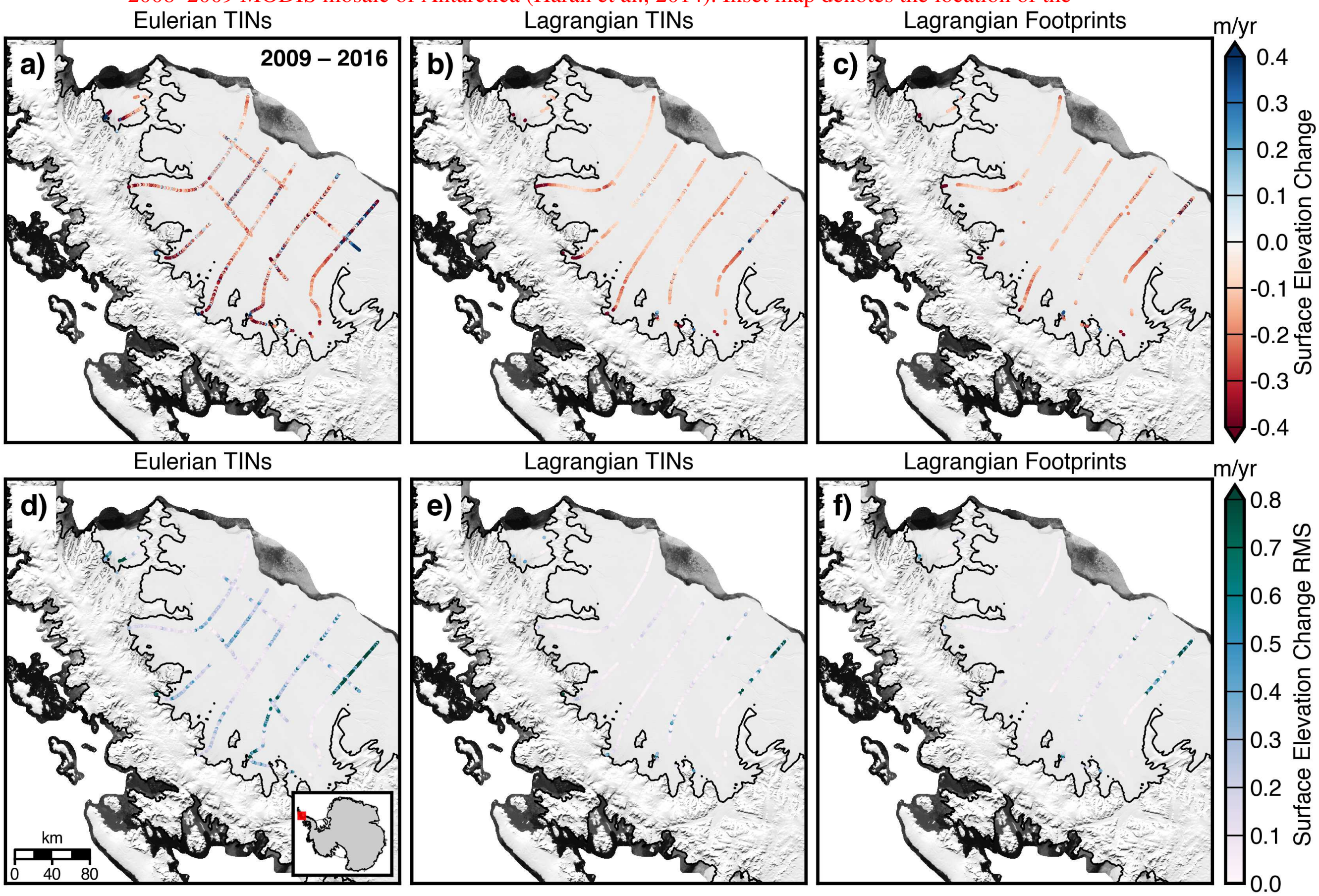

Figure 4. Surface elevation change of the Larsen-B remnant and Larsen-C Ice Shelf derived using a) Eulerian TINs corrected for strain, b) Lagrangian TINs and c) Lagrangian overlapping footprint schemes for the period 2009–2016. RMS differences in elevation change from a measurement point for all points within 1 km for the d) Eulerian TINs corrected for strain, e) Lagrangian TINs and f) Lagrangian overlapping footprint methods. The elevation change rates shown here are not RDE filtered (Smith et al., 2017). Antarctic grounded ice boundaries are provided by Mouginot et al. (2017b). Plots are overlaid on a 2008–2009 MODIS mosaic of Antarctica (Haran et al., 2014). Inset map denotes the location of the maps.

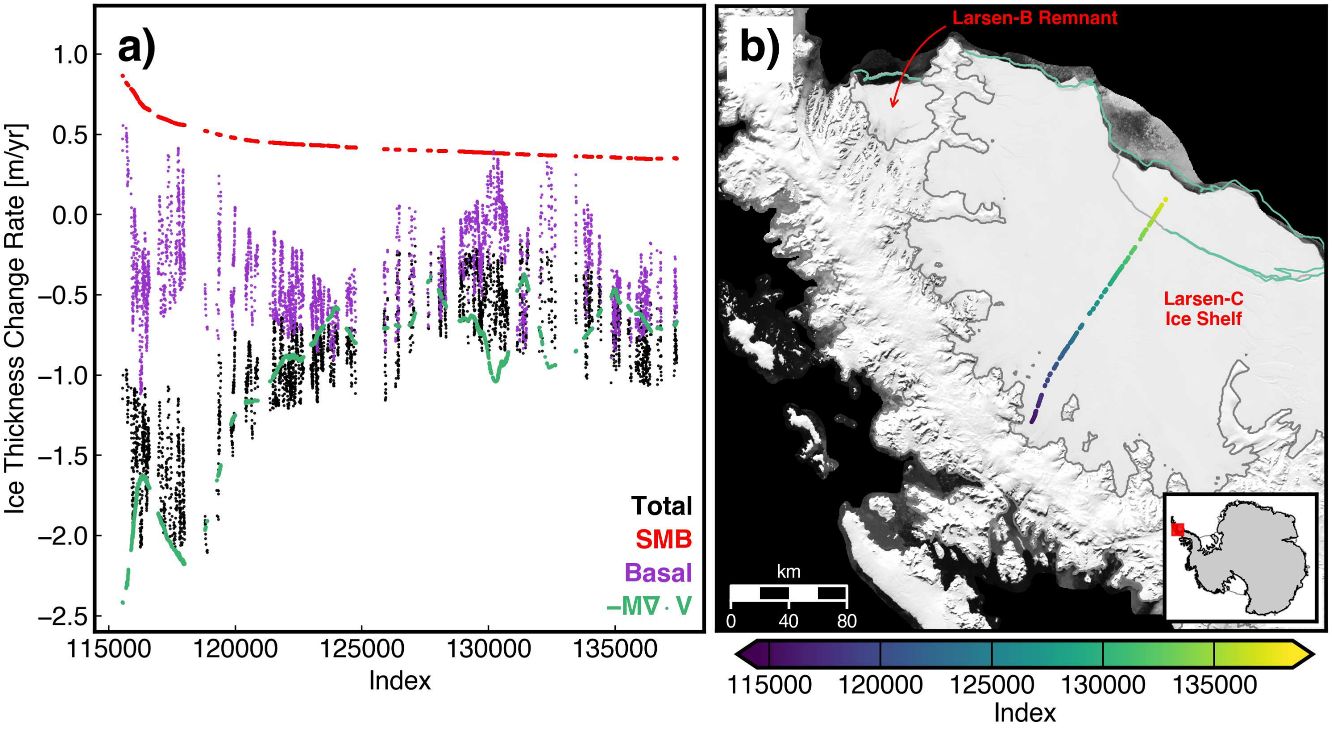

Figure 5. Measured and estimated ice thickness change rates from 2008 to 2016 for a flight line over the Larsen-C ~~ice shelf~~ Ice Shelf (a) starting near the Whirlwind inlet with the total measured ice thickness change rate denoted in black, the surface mass balance (SMB) fluxes from RACMO2.3p2 (XPEN055) denoted in red (van Wessem et al., 2016), the flux divergence terms combining ice thicknesses from Bedmap2 (Fretwell et al., 2013) and ice velocities from MEaSUREs (Rignot et al., 2017) denoted in green and the residual basal thickness change rates denoted in purple. Index denotes the ATM Icessn record number for October 10, 2008. Locations of co-registered records from the flight line are shown in b). MEaSUREs InSAR-derived Antarctic grounded ice boundaries are denoted in gray (Mouginot et al., 2017b). 2016 and 2017 ice shelf extents delineated from MODIS imagery are denoted in green and light gray respectively (Scambos et al., 2001). Map is overlaid on a 2008–2009 MODIS mosaic of Antarctica (Haran et al., 2014). Inset map denotes the location of the map.

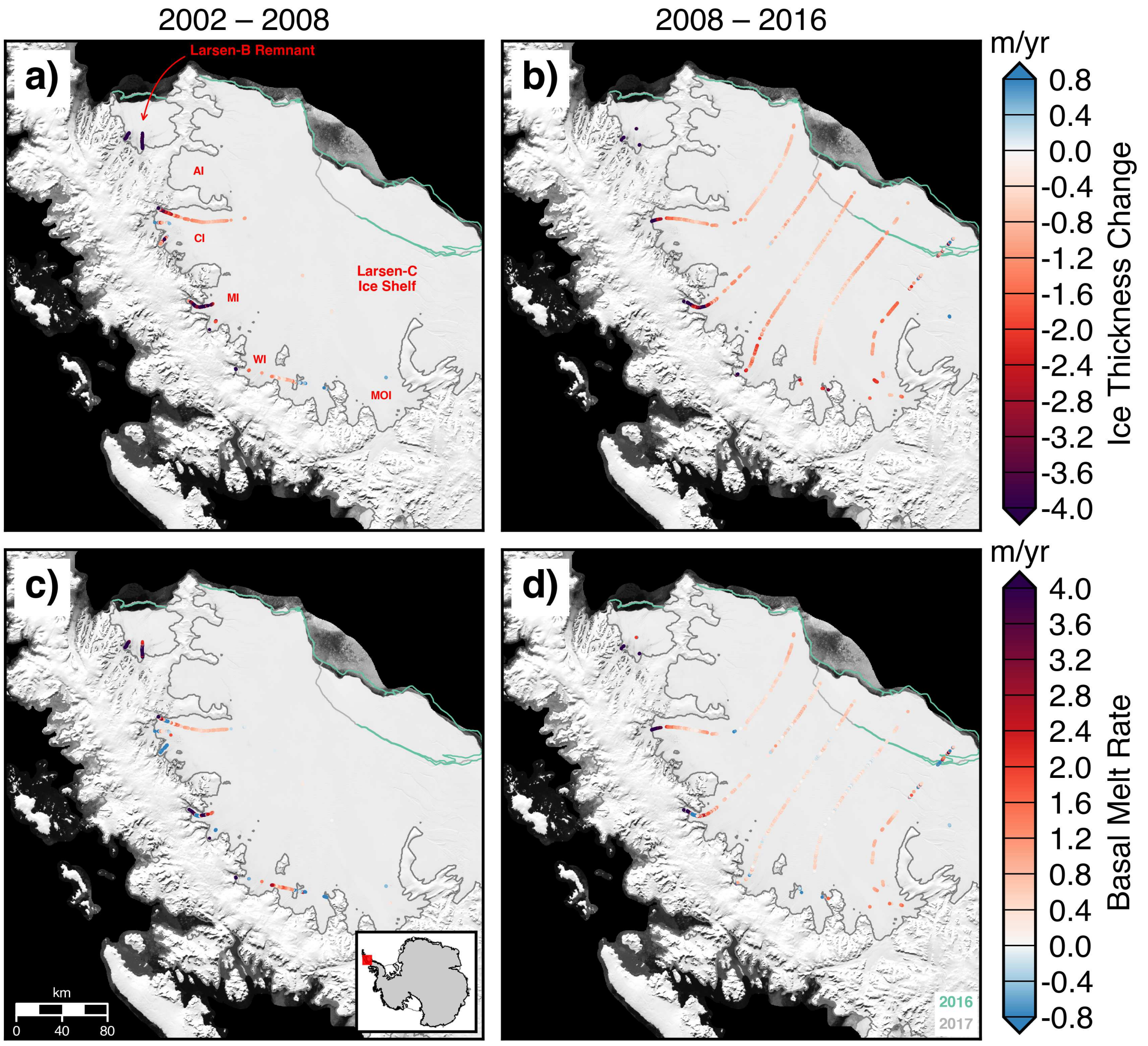

Figure 6. Ice thickness change (a-b) and estimated basal ~~thickness change~~ melt rates (c-d) of the ~~Wilkins ice shelf~~ Larsen-B remnant and Larsen-C Ice Shelf for two periods, ~~2008–2011~~ 2002–2008 and ~~2011–2014~~2008–2016. AI, CI, MI, WI and MOI denote the Adie, Cabinet, Mill, Whirlwind and Mobiloil inlets respectively. MEaSUREs InSAR-derived Antarctic grounded ice boundaries are denoted in gray (Mouginot et al., 2017b). ~~Historical~~ 2016 and 2017 ice shelf extents delineated from ~~Landsat and~~ MODIS imagery are denoted ~~with colored lines (LPDAAC; Scambos et al., 2001)~~in green and light gray respectively (Scambos et al., 2001). Plots are overlaid on a 2008–2009 MODIS ~~images~~ mosaic of Antarctica (Haran et al., 2014). Inset map denotes the location of the maps.

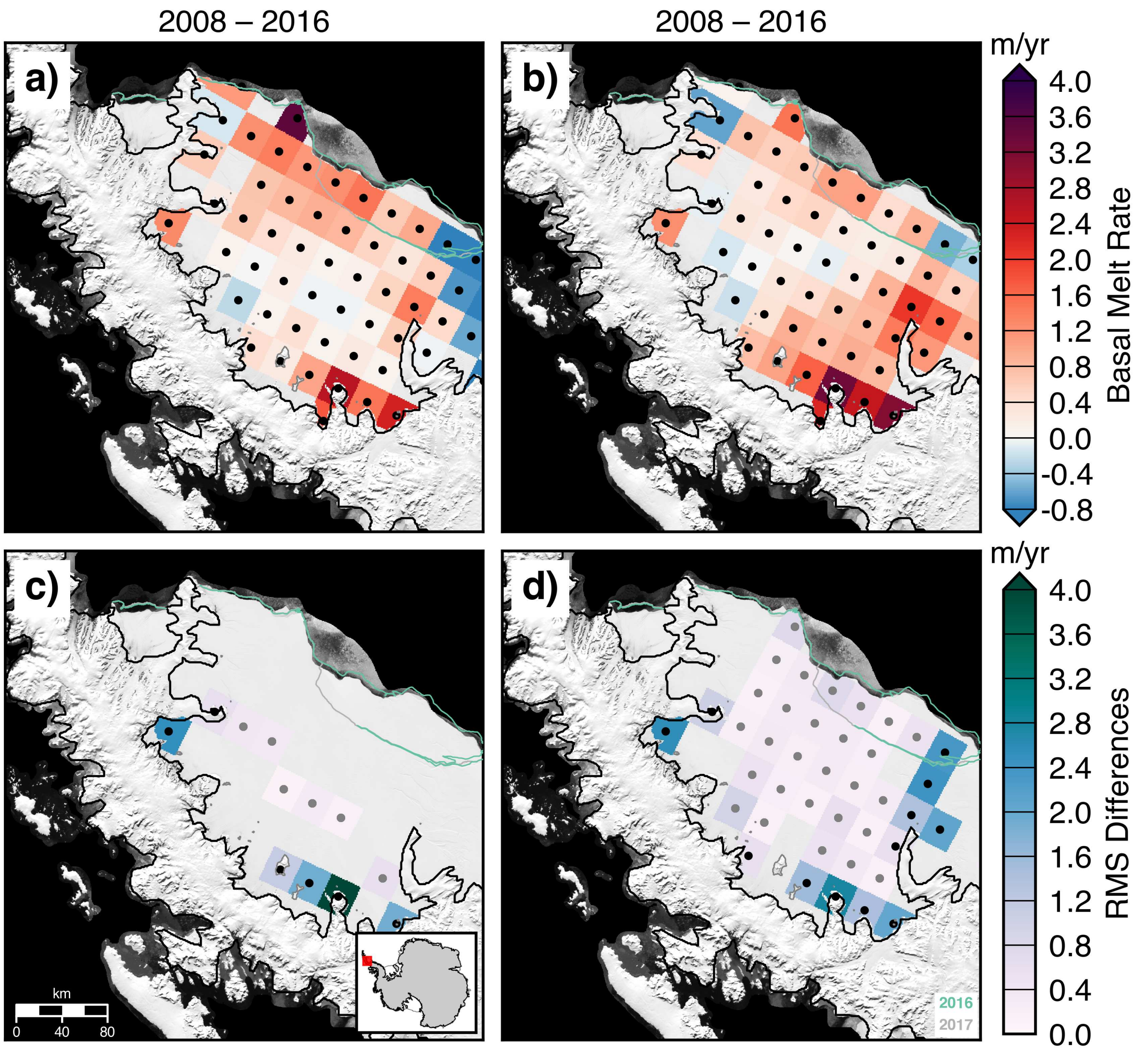

Figure 7. Estimated basal melt rates (a-b) from Adusumilli et al. (2018) and differences from melt rates derived from Operation IceBridge (c-d) of the Larsen-C Ice Shelf for two periods, 2002–2008 and 2008–2016. Stipples indicate locations with valid radar altimetry data (a-b) and coincident airborne laser altimetry data (c-d). MEaSUREs InSAR-derived Antarctic grounded ice ~~shelves provided by NSIDC~~ boundaries are denoted in gray (Mouginot et al., 2017b). 2016 and 2017 ice shelf extents delineated from MODIS imagery are denoted in green and light gray respectively (Scambos et al., 2001). Plots are overlaid on a 2008–2009 MODIS mosaic of Antarctica (Haran et al., 2014). Inset map denotes the location of the maps.

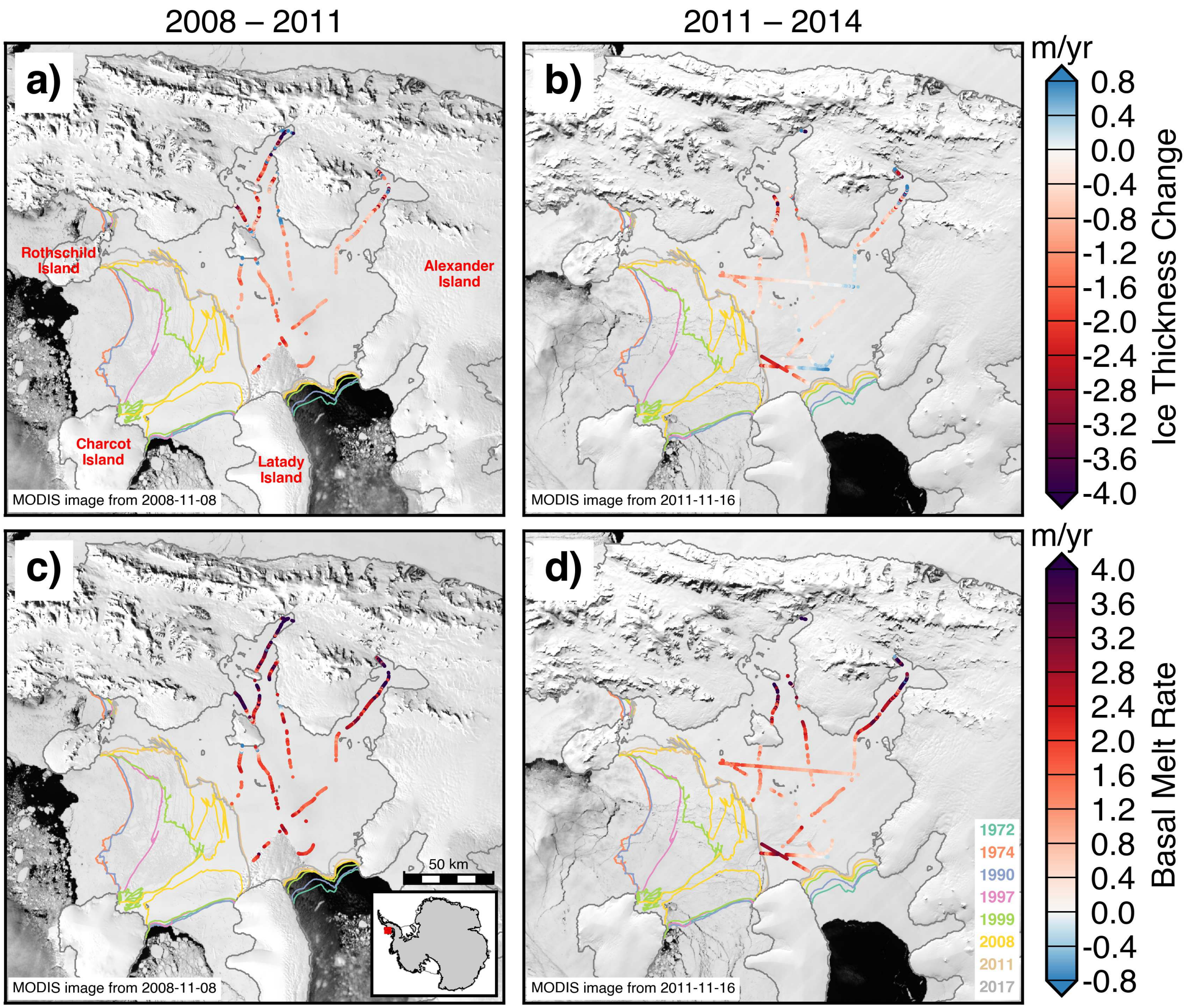

Figure 8. Ice thickness change (a-b) and estimated basal ~~thickness change~~ melt rates (c-d) of the ~~Pine Island ice shelf~~ Wilkins Ice Shelf for two periods, ~~2009–2011~~ 2008–2011 and ~~2011–2015~~2011–2014. MEaSUREs InSAR-derived Antarctic grounded ice boundaries are denoted in gray (Mouginot et al., 2017b). ~~1996 InSAR-derived grounding line locations~~ Historical ice shelf extents delineated from ~~Rignot et al. (2016)~~ Landsat and MODIS imagery are ~~delineated in green~~denoted with colored lines. Plots are overlaid on MODIS images of Antarctic ice shelves provided by NSIDC (Scambos et al., 2001). Inset map denotes the location of the maps.

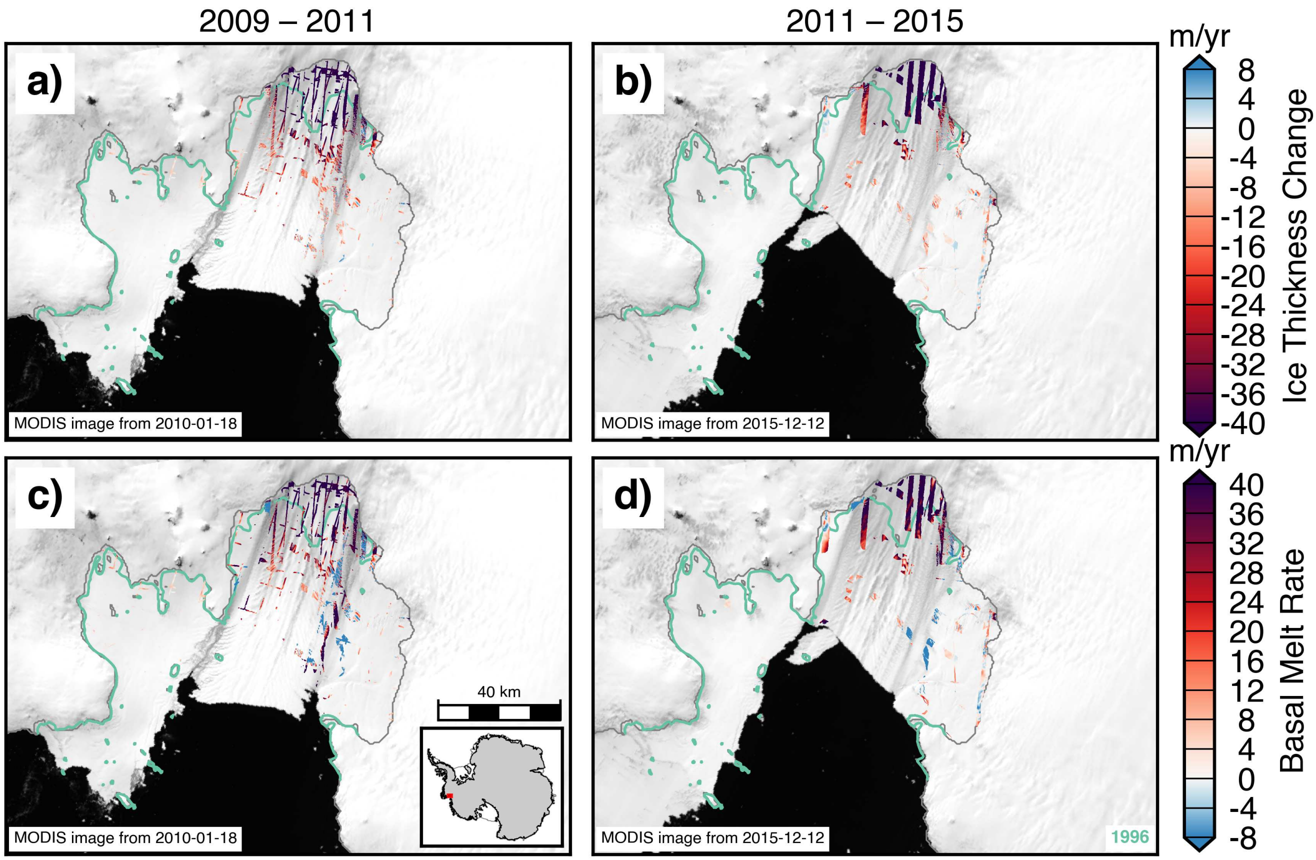

Figure 9. Ice thickness change (a-b) and estimated basal ~~thickness change~~ melt rates (c-d) of the ~~Dotson and Crosson ice shelves~~ Pine Island Ice Shelf for two periods, ~~2002–2010~~ 2009–2011 and ~~2010–2015~~2011–2015. MEaSUREs InSAR-derived Antarctic grounded ice boundaries are denoted in gray (Mouginot et al., 2017b). 1996 InSAR-derived grounding line locations from Rignot et al. (2016) are delineated in green. Plots are overlaid on ~~a 2008–2009~~ MODIS ~~mosaic~~ images of ~~Antarctica (Haran et al., 2014)~~Antarctic ice shelves provided by NSIDC (Scambos et al., 2001). Inset map denotes the location of the maps.

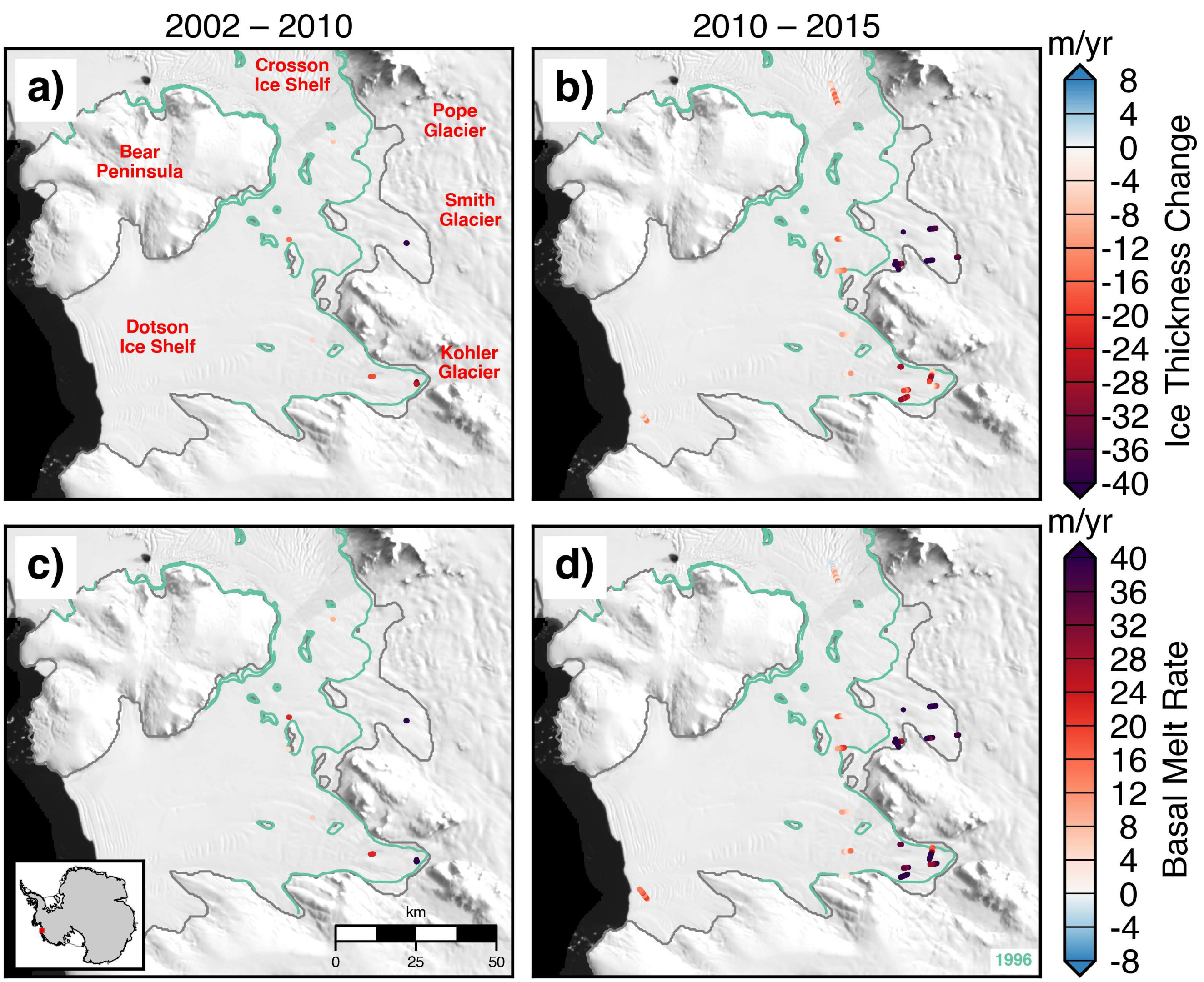

Figure 10. ~~Surface elevation~~ Ice thickness change ~~of the Larsen-B remnant and Larsen-C ice shelf derived using a~~(a-b) ~~Eulerian TINs, b) Lagrangian TINs~~ and ~~e~~estimated basal melt rates (c-d) ~~Lagrangian overlapping footprint schemes for~~ of the ~~period 2009–2016. RMS differences in elevation change from a measurement point~~ Dotson and Crosson Ice Shelves for ~~all points within 1 km for the d) Eulerian TINs~~two periods, ~~e) Lagrangian TINs~~ 2002–2010 and ~~f) Lagrangian overlapping footprint methods~~2010–2015. ~~The elevation change rates shown here are not corrected for oceanic or surface processes and are not RDE filtered (Smith et al., 2017).~~ MEaSUREs InSAR-derived Antarctic grounded ice boundaries are ~~provided by Mouginot et al. (2017b)~~denoted in gray (Mouginot et al., 2017b). 1996 InSAR-derived grounding line locations from Rignot et al. (2016) are delineated in green. Plots are overlaid on a 2008–2009 MODIS mosaic of Antarctica (Haran et al., 2014). Inset map denotes the location of the maps.